Chemical characterization and sources of submicron aerosols in the northeastern Qinghai-Tibet Plateau: insights from high-resolution mass spectrometry

Xinghua Zhang et al.

We appreciate the reviewers for their constructive comments and suggestions. The manuscript has been revised accordingly. Our point-by-point responses to the comments are presented below. The comments are in black, followed by responses in blue and revised manuscript in red with changes marked by underline.

Response to reviewer #1

A filed campaign was conducted at Waliguan Baseline Observatory (3816 m a.s.l.), the northeast edge of Qinghai-Tibet Plateau (QTP) during summer season using a high-resolution aerosol mass spectrometer to study the highly time-resolved chemistry and sources of submicron aerosols. The authors found that sulfate dominated the total PM_1 in the northern QTP whereas organic aerosols contributed more than half of the total PM_1 in the southern or central QTP, suggesting the very different aerosol characteristics and sources in different regions of QTP. Source apportionment of organic aerosol (OA) identified two relatively oxidized OAs, more-oxidized oxygenated OA (OOA) and aged biomass burning OA (agBBOA). Relatively high mass concentrations of PM_1 and enhanced contributions from sulfate and biomass burning related OA components were found for air masses from the northeast of WLG with shorter transport distance, indicating the significant impacts of regional transported aerosols from industrial areas in the northwestern China to high elevation site in the northeastern QTP. Overall, the dataset provided by this work is valuable. The manuscript is overall well written and documented. The topic fits well in the scope of ACP. I recommend this manuscript can be published after some revisions.

Thank you very much for your insightful suggestion and positive comments.

Comments:

(1) Please specify which method was used for elemental analysis, I-A or A-A?

The elemental ratios in this study were determined using the "improved-ambient" (I-A) method. We have declared this in Sect. 2.3 (Data Processing) and Sect. 3.2 (Bulk characteristics and elemental composition of OA) in the revised version. Specific descriptions are as follows.

"...to analyze the ion-speciated mass spectra, components and elemental compositions (e.g., oxygen-to-carbon (O/C), hydrogen-to-carbon (H/C), nitrogen-to-carbon (N/C) and organic mass-to-organic carbon (OM/OC) ratios using the "improved-ambient" method (Canagaratna et al., 2015)) of organics in this study."

"Note that the elemental ratios of O/C, H/C, N/C and OM/OC in this study were all determined using the "improved-ambient" method (Canagaratna et al., 2015), which increased O/C by 29%, H/C by 14% and OM/OC by 15% on average, respectively, comparing with those determined from the "Aiken ambient" method (Aiken et al., 2008) (Fig. S8)".

(2) Line 195, 0.23 should be 0.25.

Agree. We have changed this value from 0.23 to 0.25 in the revised version. The organic fragmentation in this study was used from the default values. We also rewrote this sentence as follows in the revised version.

"For example, the signals of H_2O^+ and CO^+ for organics were scaled to that of CO_2^+ as $CO^+ = CO_2^+$ and $H_2O^+ = 0.225 \times CO_2^+$, while signals of HO^+ and O^+ were set as $HO^+ = 0.25 \times H_2O^+$ and $O^+ = 0.04 \times H_2O^+$ according to Aiken et al. (2008)."

(3) The description of geographic orientation in the manuscript need to be checked and revised carefully, especially the usage like north/northern, northeast/northeastern, etc. The right usage should to be "in the northeast edge of QTP" or "in the northeastern QTP" rather than "in the northeastern edge of QTP" or "in the northeast QTP".

Agree. We have checked and revised carefully in the revised manuscript as follows.

"at the northeast edge of Qinghai-Tibet Plateau (QTP)"

"in the northeast part of QTP "

"in the central or southern QTP"

(4) One of the highlights in this study was the unique aerosol chemical characteristics at WLG compared with other highland sites in the central or southern QTP. Can the author present some direct comparisons via tables or figures besides the simple description in sentences?

Thanks for the reviewer's suggestion. A new graph has been added in the supplementary information (Figure S1) to show the comparison of aerosol chemical characteristics among various field studies that conducted at high elevation sites in the QTP. The specific modification in the revised manuscript and Figure S1 added to the supplementary information are shown as follows.

"In recent years, the deployments of AMS in the highland areas of QTP have been conducted in a few field studies (Fig. S1), including..."

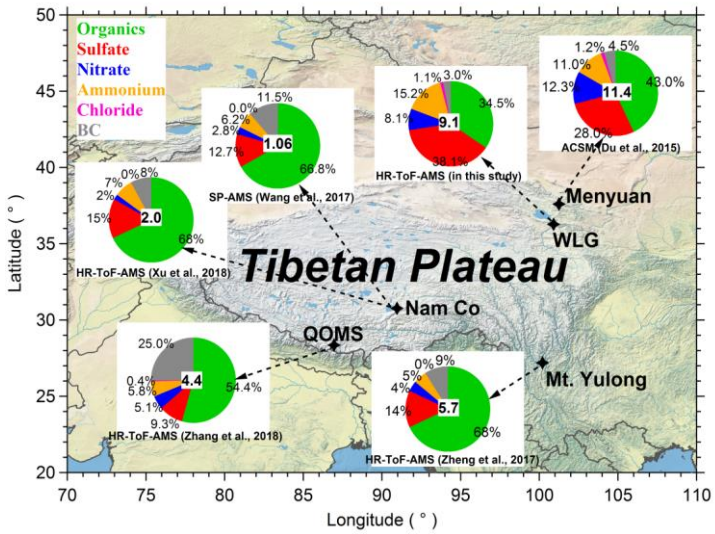

Figure S1. The field studies conducted at high elevation sites in the Qinghai-Tibet Plateau using AMS or ACSM measurements. The mass concentrations of PM_1 and the mass contributions of each chemical species (pie chart) are presented in each site.

(5) Line 62-63, "due to the influence of anthropogenic emissions from inland of northwest China". The expression of "inland of northwest China" is incorrect and need to be changed to "...from industrial areas in the northwestern China". Similarly, lines 472 and 488.

Agree. We have made changes to the three lines in the revised manuscript as follows.

"...due to the influence of anthropogenic emissions from industrial areas in the northwestern China"
"...indicating the apparently regional transport of sulfate from industrial areas in the northwestern China"
"...mainly due to the enhanced contributions of sulfate and biomass burning related OA components from the industrial areas in the northwestern China"

(6) Line 68, change "strongly" to "strong".
Corrected.

(7) Line 73-74, "in the northeastern QTP " moved after "aerosol particles".
Corrected.

(8) Line 81, delete "species".
Corrected.

(9) Line 96, the expression of "long-range transport biomass burning emissions" was used several times in the whole manuscript, however, it seemed inappropriate and could be changed to "long-range transported biomass burning emissions".
Thanks a lot for the reviewer's suggestion. The expressions of "long-range transport" are used several times in the whole manuscript, however, only those used as adjective are changed to "long-range transported", whereas those used as noun are still as "long-range transport" in the revised version. For example,
"...for observing the natural background aerosol and long-range transported aerosol"
"...indicating the well mixed and highly aged aerosol particles at WLG from long-range transport"

(10) Line 117, the expression of "GongHe county" need to be changed to "Gonghe county", consistent with that of "Xining".
Corrected.

(11) Line 253-256, this sentence is too long and confusing, please rewritten.
We have rewritten this long sentence into two short sentences in the revised version as follow.
"Bulk acidity of PM_1 at WLG was also evaluated according to the method in Zhang et al. (2007). The predicted ammonium was calculated based on the mass concentrations of sulfate, nitrate and chloride and assumed full neutralization of these anions by ammonium."

(12) Line 274-275, Figure 3c, the scales of y-axis for the size distributions of organics and three inorganic species are not consistent. It is difficult to conclude that "organics presented relatively wider distribution than the three secondary inorganic species in the small sizes".
Thanks for the reviewer's insightful suggestion.
We have modified Figure 3c in the revised version. In Figure 3c, it is clear that OA present a relatively wider distribution than the other three secondary inorganic species in the small sizes (< 300 nm).

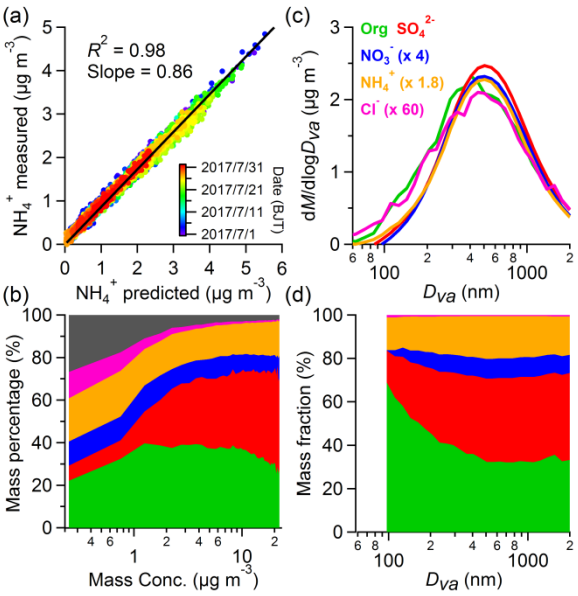

Figure 3. (a) Scatterplot and linear regression (black solid line) of measured NH_4^+ versus predicted NH_4^+ based on the mass concentrations of SO_4^{2-}, NO_3^-, and Cl^-, **(b)** the mass contributions of PM_1 chemical species as a function of total PM_1 mass concentration, and the average size distributions of **(c)** mass concentrations and **(d)** mass contributions of NR-PM_1 species in this study.

(13) Line 329, "... in previous studies", please add the references.

We have added the corresponding references in the revised version as follows.

"Similar to several HOA mass spectra reported in previous studies (Zhang et al., 2005; Ng et al., 2011), HRMS of HOA in this study was also dominated by hydrocarbon ion series..."

(14) In Figure S9, the author shows the scatter plots of the comparisons between the four high-resolution mass spectra identified in this study and those determined from other studies. Are they HMR or UMR spectra?

All the mass spectra in Figure S11 in the revised version (corresponding to Figure S9 in previous version) are HMR. We have clarified this point in the manuscript and supplementary information, respectively.

"Besides, the high-resolution mass spectrum of HOA was highly similar to those from other locations around the world..."

"Figure S11. Scatter plots of the comparisons between the four high-resolution mass spectra identified in this study and those high-resolution mass spectra determined from other studies."

(15) Line 342-343, please explain more on the diurnal variation of HOA at WLG site.

We have added a specific explanation on the diurnal variation of HOA in the revised version as follows.

"Although there was not traffic rush hour in the high-elevation site, the increasing vehicles on the national road combined with the valley breeze together lead to the slightly higher HOA concentrations in the late morning, then HOA decreased continuously with the increasing planetary boundary layer (PBL) height in the afternoon and elevated again to a stable high level during the nighttime due to the low PBL height and mountain breeze."

(16) Line 401, the expression of "PBL variation" is inappropriate and needs to be rewritten.

We have rewritten this sentence as follows.

"Although OOA showed relatively stable contributions throughout the whole day, the OOA mass concentrations also presented distinct diurnal variation at WLG site, namely relatively low values in the late morning, continuously increasing trend during the afternoon and moderate values at the nighttime (Fig. 6c and d), which was tightly associated with the photochemical activities in the daytime, aqueous-processing of OA at nighttime as well as the diurnal variation of PBL height."

Response to reviewer #2

This paper reports on the chemical characterization and sources of submicron aerosols observed at Waliguan Baseline Observatory, a high-altitude background station in the northeastern Qinghai-Tibet Plateau (QTP), during summer season using a high-resolution time-of-flight aerosol mass spectrometer (HR-ToF-AMS) along with other online instruments. Mass concentrations and fractions of PM_1 chemical species, bulk aerosol acidity and size distribution are characterized, respectively. The PM_1 mass in the northeastern QTP is obviously higher than those at other high-elevation sites in the southern or central QTP and sulfate dominates the total PM_1, which relates tightly with the regional transport of intense industrial emissions from areas in the northwestern China. Four distinct OA components, including two biomass burning related OAs with different oxidation degree as well as one oxygenated OA and one traffic related OA, are identified by the PMF analysis. Source analysis finally show that the prevailing air masses from northeast with lower transport height and distance can bring surface anthropogenic and industrial pollutants to Mt. Waliguan. Overall, this paper adds new and valuable measurements of aerosol compositions and concentrations in the northeastern QTP, one of the less studied key regions. The paper is within the scope of ACP and generally well written. I recommend publication of this paper in ACP after revisions. I only have some minor points for the author to consider in the revision.

We thank the reviewer for his/her careful review of the manuscript.

Comments:

(1) The full expression need to be added when the abbreviations are used first time in the manuscript, such as NO_x, PM_{10}, and PBL, etc..

Thanks for the reviewer's suggestion. We have checked the manuscript carefully and added the full expressions to all of the abbreviations when they are used at the first time as follows.

"Nitrate, oxidized from the nitric oxides (NO_x), was also an important component in the northern QTP..."

"...including the mass concentrations of $PM_{2.5}$ and PM_{10} (particulate matter with diameter less than 10 μm) measured by a TEOM 1405-DF dichotomous ambient particulate monitor with a filter dynamics measurement system (Thermo Scientific, Franklin, MA, USA) and gaseous pollutants of carbon monoxide (CO) and ozone (O_3) measured using the Thermo gas analyzers..."

"This conclusion could be further demonstrated by the emission distribution of sulfur dioxide (SO_2) in China observed by the Ozone Monitoring Instrument (OMI) satellite data in previous studies"

"...then HOA decreased continuously with the increasing planetary boundary layer (PBL) height in the afternoon..."

(2) Line 171, does the OM/OC here refer to organic mass or organic matter?

The OM/OC in this study refer to the ratio of organic mass to organic carbon. The definition of OM/OC added in the revised version is shown as follows.

"to analyze the ion-speciated mass spectra, components and elemental compositions (e.g., oxygen-to-carbon (O/C), hydrogen-to-carbon (H/C), nitrogen-to-carbon (N/C) and organic mass-to-organic carbon (OM/OC) ratios using the "improved-ambient" method (Canagaratna et al., 2015)) of organics in this study."

(3) Although the AMS mass spectrometer in this study was toggled between V-mode and W-mode every 5 min and the W-mode was used to obtain the high resolution mass spectral data for PMF analysis (in Line 160-165), the author also state in Line 188-190 that the data and error matrices input into the PMF analysis were finally generated from V-mode data rather than W-mode due to the low aerosol mass loading at WLG, hence the entire data used in this study for mass concentration, size distribution and PMF analysis are all from V-mode with 10-min time resolution rather than 5-min, please checked and revised totally.

We thank the reviewer for your insightful suggestion. The data time resolution in this study is indeed 10-min rather than 5-min because we do not use the W-mode data due to the low aerosol mass loading in the QTP. We have rewritten this sentence as follows.

"Similar to most of the previous AMS field measurements, the mass spectrometer was toggled under the high sensitive V-mode (detection limits ~ 10 ng m^{-3}) and the high resolution W-mode (~ 6000 m/Δm) every 5 min in this study. Under the V-mode operation, the instrument also switched between the mass spectrum (MS) mode and the particle P-ToF mode every 15 s to obtain the mass concentrations and size distributions of NR-PM_1 species, respectively, whereas the high resolution W-mode was used to obtain high resolution mass spectral data. However, the data and error matrices inputted into the PMF analysis were finally generated from the V-mode data rather than the W-mode data in this study due to the low aerosol mass loading at WLG. Hence, all the data used in this study are from V-mode with 10 min time resolution."

(4) Line 216, when the unique burning event occurred and why was it removed?

The unique burning event mentioned in this study was a local Tibetan festival event occurred during 5−6 July 2017. During the festival, hundreds of local Tibetans gathered together from the evening of 5 July till the late morning of next day to worship their religious god by burning large amounts of specific biofuels when chanting around the pagoda. The emissions from these hundreds of vehicles and motorcycles and biomass burning activities together led to an extraordinary air pollution condition around the study site. Intense burst of aerosol emissions occurred at the midnight on 5 July, with the mass concentration of PM_1 increased significantly from less than 10 μg m^{-3} at 23:00 BJT on 5 July to the maximum value of 232 μg m^{-3} at 01:30 BJT on 6 July. Hence, the extremely high aerosol mass loadings during the event can impact on the average results of field measurement and need to be removed. We also have added a specific introduction to this unique burning event in the revised version as follow.

"The missing data are due to hardware or software malfunction, maintenance of the instrument, or removing large spikes and unique burning event (a local Tibetan festival event occurred during 5−6 July 2017 with extremely high aerosol mass loadings) in data processing."

(5) Line 239, the author explained the high mass concentration at WLG was due to the relatively shorter distance from the polluted city center and strongly mountain-valley breeze during summer,

are there any other evidences to support this conjecture? Such as references, WD variations or air mass trajectories.

As mentioned in the manuscript, the PM_1 mass concentration at WLG (9.1 μg m^{-3}) in the northeastern QTP was much higher than those at NamCo (2.0 μg m^{-3}) in the central QTP and QOMS (4.4 μg m^{-3}) in the southern QTP. We compared the air mass trajectories at WLG during July 2017 in this study with those at NamCo during June 2015 in Xu et al. (2018) and QOMS during April-May 2016 in Zhang et al. (2018) (Figure R1). Clearly predominant northeastern winds (57%) with shorter transported distance and lower transported height were found at WLG in this study, whereas long-range transported air masses from south Asia dominated apparently at Nam Co Station and QOMS. We have added a specific explanation in the revised manuscript as follow.

"The higher PM_1 mass concentration at WLG in the northeastern QTP comparing with those at other sites in the central or southern QTP was likely due to the relatively shorter distance from the industrial areas (e.g., Xining city) in the northwestern China and strong mountain-valley breeze during summer. This conclusion could be supported by the comparisons of air mass back-trajectories between WLG in this study (see Sect. 3.4 for details) and those at Nam Co Station in Xu et al. (2018) and QOMS in Zhang et al. (2018)."

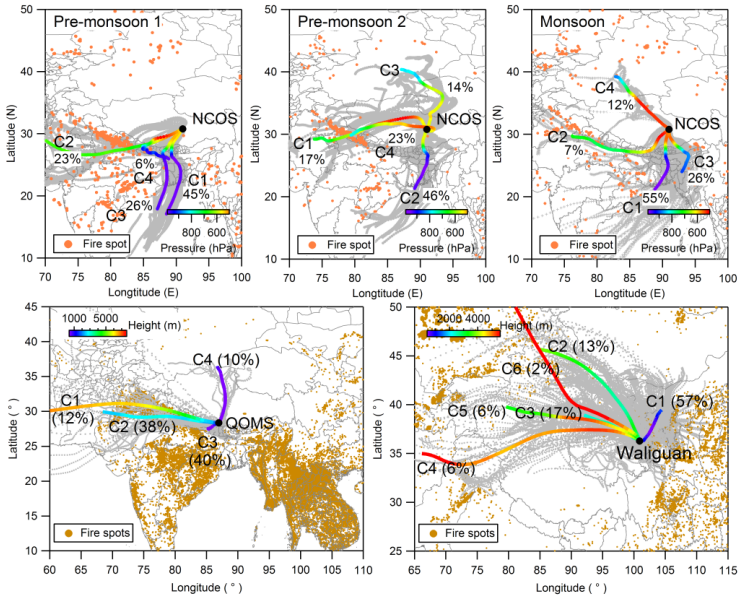

Figure R1. Air mass back trajectories at WLG in this study comparing with those at Nam Co Station (NCOS) in Xu et al. (2018) and QOMS in Zhang et al. (2018).

(6) Line 290, are there any other ion fragments at m/z 44? Please checked carefully for those similar expressions in the whole manuscript.

We have checked carefully according to the reviewer's suggestion. The ion at m/z 44 is only CO_2^+ in this study and only $C_2H_4O_2^+$ at m/z 60. We have rewritten those corresponding sentences in the revised version.

"...with significantly high contribution at *m/z* 44 (17.9%; composed totally by CO_2^+ in this study and similarly hereinafter)"

(7) Line 293, "at Lanzhou, an urban city located at the northeastern edge of QTP". The description of Lanzhou that located at the northeast edge of QTP seemed inappropriate.

We have deleted this description.

(8) Line 308-313, these sentences for diurnal variations of elemental ratios need to be rewritten clearly.

Thanks for the reviewer's suggestion. We have rewritten these sentences in the revised version. Specific changes are as follows.

"The relatively higher O/C and OM/OC during afternoon potentially related with the photochemical oxidation processes in the daytime, while lower values in the late morning mainly associated with the transport of relatively fresh OA from nearby areas to WLG site, which could be further revealed by the corresponding higher H/C and N/C ratios in the late morning as well as the diurnal variations of the two primary OA components (see Sect. 3.3 for details)."

Technical Comments:

(1) Line 39-41, "Its huge surface area...and therefore called as the third pole". These are two sentences with different subject, please rewritten.

Agree. We have made changes to this sentence in the revised version.

"Its huge surface area (~ 2,500,000 km^2) and high elevation (with a mean elevation of more than 4000 m above sea level (a.s.l.)) make it especially important in earth sciences and therefore the QTP is generally called as the "third pole" (Yao et al., 2012)".

(2) The tense in one sentence should consistent, please check the entire manuscript carefully, e.g., Line 48-49, "climb" and "move" need to be changed to "climbed" and "moved", respectively.

Thanks for the reviewer's suggestion. We have checked the entire manuscript carefully to make the tense consistent in the manuscript.

(3) Line 55, change "that in the southern QTP" to "those in the southern QTP".

Corrected.

"...aerosol particles in the northern QTP showed quite different behaviors comparing with those in the southern QTP..."

(4) Line 57, change "however" to "nevertheless".

Agree.

"For example, Li et al. (2016) found equal important contributions from fossil fuel (46%) and biomass (54%) aerosol sources to BC in the Himalayas, nevertheless, it was dominated by fossil fuel combustion (66%) in the northern QTP."

(5) Line 59, change "distinct" to "distinctly".

We have checked the entire manuscript carefully to make sure the expressions like this are used correctly.

"Correspondingly, the chemical composition of ambient aerosol in the northern QTP was also distinctly different with that in the southern QTP."

(6) Line 62, change "sulfate was a..." to "sulfate was the".

Agree.

"...and found sulfate was the dominant component during summer season..."

(7) Line 83, change "high attention to" to "great concern of".

Corrected.

"AMS has been widely implemented worldwide in recent decades, especially in China since 2006 due to the great concern of atmospheric environment"

(8) Line 87, add "the" before "deployment".

Corrected.

"In recent years, the deployments of AMS in the highland areas of QTP have been conducted in various field studies..."

(9) Line 90-91, change "a HR-ToF-AMS at QOMS (Zhang et al., 2018) and Mt. Yulong (Zheng et al., 2017) in the southern QTP" to "a HR-ToF-AMS at QOMS in the southern QTP (Zhang et al., 2018) and a HR-ToF-AMS at Mt. Yulong in the southeastern QTP (Zheng et al., 2017)".

Thanks for the suggestion. We have made changes as following in the revised version.

"a HR-ToF-AMS at QOMS in the southern QTP (Zhang et al., 2018) and a HR-ToF-AMS at Mt. Yulong in the southeastern QTP (Zheng et al., 2017)"

(10) Line 224, "daily mean values" change to "daily mean precipitation" and the unit must be mm d^{-1} rather than mm d^{-3}.

We made a mistake here and revised it as follows.

"...with daily mean precipitation of 2.6 and 7.4 mm d^{-1}, respectively "

(11) Line 230, add "the" before "average".

Corrected.

"Overall, the average mass concentration of total PM_1 (± 1σ) at WLG for the entire study was 9.1 (± 5.3) μg m^{-3}..."

(12) Line 238, the sentence of "The high mass concentration at WLG..." need to be rewritten, because the mass concentration is just relatively higher when comparing with other sites in the QTP yet much lower than those at other urban or rural sites in China.

Thanks a lot for the reviewer's suggestion. We have rewritten this sentence clearly to avoid ambiguity.

"The higher PM_1 mass concentration at WLG in the northeastern QTP comparing with those at other sites in the central or southern QTP was likely due to..."

(13) Line 278, change "contributed" to "contribute".

Corrected.

"Specifically, organics could contribute more than half of the ultrafine NR-PM_1..."

(14) Line 307, change "suggesting an overall regional transport organic aerosol source at WLG" to "suggesting an overall OA source from regional transport at WLG".

Corrected.

(15) Line 320, change "HRMS of OA" to "OA HRMS".

Corrected.

"PMF analysis on the OA HRMS identified four distinct components..."

(16) Line 355, change "high" to "higher".

Corrected.

"Correspondingly, the $C_xH_yO_z^+$ fragment also showed higher contribution for agBBOA than that for BBOA..."

(17) Line 367, "spectrums" change to "spectra".
Corrected.
"...with other standard BBOA mass spectra at other sites around the world..."

Response to reviewer #3

This paper presents near real time high resolution aerosol measurements, looking at the chemical composition and sources of organic aerosols. The measurements were taken at a high-altitude background site, northeast of Qinghai-Tibet Plateau, July 2017. The authors found SO_4 to dominate PM_1 concentrations and identified four different OA sources after PMF analysis. The research presented in this paper will help to better understand OA chemical composition and sources. Overall, the manuscript is well written with a good work on the use of references. The paper, which fits well within the scope of ACP, is recommended to be published after working on the following minor comments.
Thank you very much for your insightful suggestion and positive comments.

Comments:
(1) Page 2 line 60. Rephrase it, i.e. conducted aerosol composition studies.
We have rephrased this sentence according to the reviewer's comment.
"Xu et al. (2014a, 2015) conducted aerosol composition studies from filter measurements..."

(2) Page 2 line 63. Rephrase it, i.e.: Similar results were also found by Li et al.
Agree. We have changed "found in Li et al." to "found by Li et al." in the revised version.
"Similar results were also found by Li et al. (2013) and Zhang et al. (2014) which conducted field studies in the northeast part of QTP."

(3) Page 2 line 69. Check and rephrase the following paragraph: In addition, air pollutants to the northern QTP could also from the central Eurasian continent where locates in the upstream of the northwest of China, although relatively lower air masses presented comparing with those impacted by anthropogenic emissions from China and the Indian subcontinent (Xue et al., 2013).
We have rewritten this sentence as follows.
"Besides the significant impacts by anthropogenic emissions from the northwestern China or Indian subcontinent, air pollutants to the northeastern QTP could also from the central Eurasian continent (Xue et al., 2013)."

(4) Page 2 line 77. Rephrase the following paragraph: The real-time measurement of atmospheric aerosol chemistry with high time resolution is still relatively rare in the northern QTP until now.
We have rephrased the sentence as following according to the reviewer's comment.
"Studies focused on the atmospheric aerosol chemical compositions in the northeastern QTP using the high-time-resolution real-time measurements are still relatively rare until now."

(5) Page 3 line 79. Not all AMS instrument provide size distribution.
We have rewritten this sentence in the revised version.
"The Aerodyne aerosol mass spectrometer (AMS) is a unique instrument which can provide ~~both~~ chemical composition and/or size distribution information of non-refractory submicron aerosol

(NR-PM_1) with high time resolution and sensitivity (Jayne et al., 2000; Jimenez et al., 2003; Canagaratna et al., 2007)."

(6) Page 3 line 84. Change to “References therein”.

Corrected.

"AMS has been widely implemented worldwide in recent decades, especially in China since 2006 due to the great concern of atmospheric environment (Li et al., 2017, and references therein)."

(7) Page 3 line 86. Change to “Detection limit”.

Corrected.

"...AMS has also been successfully deployed at many remote sites due to its low detection limit (Fig. S1)."

(8) Page 3 line 112. Change to “is located at the top”

We have changed "which locates in the top" to "which is located at the top" in the sentence.

"...which is located at the top of Mt. Waliguan "

(9) Page 4 line 125 Change to “Aerosol measurements” or rephrase it.

We have changed "Aerosol particle measurements" to "Aerosol measurements" in the revised version.

"Aerosol measurements were performed at "

(10) Section 2.2 Instrumentation. It would be good to add the sampling time of all the instruments.

Thanks for the suggestion. All the data in this study measured by HR-ToF-AMS, SMPS, CCN or other synchronous instruments are all from 1 to 31 July 2017. We have rephrased the sentences in the "Section 2.2 Instrumentation" clearly in the revised version.

"Aerosol measurements were performed at the top floor of the main two-story building at WLG observatory from 1 to 31 July 2017 with a suit of real-time instruments, including..."

"Simultaneously, other synchronous data were also acquired at the WLG baseline observatory during the sampling period, including..."

(11) Page 6 lines 202-208. I would move this paragraph to either results or supplement as it is part of results.

Thanks for the suggestion. In our opinion, this paragraph is still belonging to the method part about PMF analysis in "Sect. 2.3 Data processing". The paragraph is used to detail the key diagnostic plots of PMF results for this study, and to illustrate the reason why we selected the four-factor solution finally via examining the model residuals, scaled residuals, Q/Q_{exp} contributions for each m/z and time, and other factors. Hence, this paragraph is better to be placed in the method part.

"A summary of the key diagnostic plots of PMF results for this study is presented in Fig. S3. Overall, the PMF solutions were investigated from one to six factors with the rotational parameter (*f*Peak) varying from −1 to 1 with a step of 0.1. Finally, a four-factor solution with *f*Peak = 0 was chosen in this study by examining the model residuals, scaled residuals and Q/Q_{exp} contributions for each *m*/*z* and time, as well as comparing the mass spectra of individual factor with reference spectra and the time series of individual factor with external tracers. The mass spectra, time series, and diurnal variations of PMF results from three-factor and five-factor solutions were also shown

in Fig. S4 and S5 for comparison, respectively. The three-factor solution did not separate the two biomass burning factors whereas the five-factor solution showed a splitting factor."

(12) Page 8 line 283. What is the purpose of comparing these two methods? And/or what is the reason of the increased ratios?

The Aerodyne HR-ToF-AMS is widely used to measure the OA elemental composition which can provide useful constraints for understanding aerosol sources, processes, impacts, and fate, and for experimentally constraining and developing predictive aerosol models on local, regional, and global scales (Canagaratna al., 2015). For the previous AMS studies commonly using "Aiken-Ambient" method, the H_2O^+ and CO^+ ion intensities was empirically estimated rather than directly measured to avoid the gas phase air interferences from gaseous N_2 and H_2O, namely the H_2O^+/CO_2^+ and CO^+/CO_2^+ ratios were empirically estimated from limited ambient OA measurements available at the time to be 0.225 and 1, respectively (Aiken et al., 2008; Canagaratna al., 2015). However, this method produced larger biases for alcohols and simple diacids (Canagaratna al., 2015). A detailed examination of the H_2O^+, CO^+, and CO_2^+ fragments in the high-resolution mass spectra of the standard compounds indicates that the "Aiken-Ambient" method underestimates the CO^+ and especially H_2O^+ produced from many oxidized species (Canagaratna al., 2015). The "Improved-Ambient" method performed by Canagaratna al. (2015) used specific ion fragments as markers to correct for molecular functionality-dependent systematic biases, namely $O/C_{I\text{-}A} = O/C_{A\text{-}A} \times (1.26 - 0.623 \times f_{CO2+} + 2.28 \times f_{CHO+})$ and $H/C_{I\text{-}A} = H/C_{A\text{-}A} \times (1.07 + 1.07 \times f_{CHO+})$. The Improved-Ambient elemental ratios are expressed as a product of Aiken-Ambient elemental ratios and a composition-dependent correction factor, which allows for simple recalculation of the Improved-Ambient elemental ratios from Aiken-Ambient values without the need for performing a re-analysis of the raw mass spectra and can be easily applied to already published AMS results (Canagaratna al., 2015).

Therefore, it was quite important to present both the elemental ratios from the two methods in recent AMS studies, which can be easily used to compare with those ratios from either previous AMS studies using "Aiken-Ambient" method or recent AMS studies using "Improved-Ambient" method. Besides, as mentioned above, the increased ratios using the "Improved-Ambient" method are mainly due to the underestimation of CO^+ and H_2O^+ using "Aiken-Ambient" method.

(13) Page 9 line 362. Change to “correlated”.

Agree. We also checked the entire manuscript carefully and corrected the similar issue at other sentences.

"As shown in the Fig. 5, the time series of agBBOA correlated tightly with $C_2H_4O_2^+$ (R^2 = 0.79) and sulfate (R^2 = 0.47), while BBOA correlated slightly weak with $C_2H_4O_2^+$ (R^2 = 0.47) and potassium (R^2 = 0.30), respectively. The time series of agBBOA also correlated well with $C_xH_yO_1^+$ and $C_xH_yO_2^+$ ions, while BBOA correlated well with $C_xH_y^+$ and $C_xH_yO_1^+$ (Fig. S9)."

"In addition, the time series of OOA also correlated well with..."

(14) Page 9 line 362. I would not say that BBOA correlated well with $C_2H_4O_2^+$ with R^2 = 0.3.

Thanks for the reviewer's suggestion. We have rephrased this sentence in the revised version.

"As shown in the Fig. 5, the time series of agBBOA correlated tightly with $C_2H_4O_2^+$ (R^2 = 0.79) and sulfate (R^2 = 0.47), while BBOA correlated slightly weak with $C_2H_4O_2^+$ (R^2 = 0.47) and potassium (R^2 = 0.30), respectively."

Technical comments.

(1) A small paragraph about OA sources in these type of sites could be added to the introduction. There is not introduction about OA sources while this topic is the focus of this paper.

We have added a small paragraph about the OA sources in the high-altitude sites in the QTP to Introduction section in the revised version as follows.

"In addition to the low PM_1 (NR-PM_1 + BC) mass loadings, the dominant contribution from organic aerosol (OA) (54−68%) was found in the southern and central QTP (Zheng et al., 2017; Wang et al., 2017; Xu et al., 2018; Zhang et al., 2018). OA was composed by oxygenated OA (OOA) and biomass burning related OA (BBOA) components in those high-altitude background sites. The OOA component was associated with the intense oxidation processes that converted fresh OA to secondary OA, while BBOA was related to the direct emissions from the biomass burning activities in the highland areas. However, relatively few studies have been conducted in the northern QTP except a measurement using Aerodyne aerosol chemical speciation monitor (ACSM) at Menyuan (Du et al., 2015)."

(2) In the mass spectra shown in figure 5, the mass spec agBBOA looks like a semi-volatile OA. More details could be added, perhaps to the supplement, about the analysis mentioned in lines 359-361 to confirm the presence of BBOA, someone would argue you can see a BBOA in summer and it could be more questionable the fact that you are identifying two types of BBOA. A few lines supporting these two BBOA profiles are suggested.

Thanks for the reviewer's insightful suggestion and we have rephrased this entire paragraph clearly in the revised version. The responses to the comment are separated into four parts as follows.

The confirmation of the presence of BBOA in this study was mainly on the basis of the *m/z* 60 signals or f_{60} values in the HRMS. According to the previous AMS studies (Cubison et al., 2011; Zhou et al., 2017), if the f_{60} values was significantly larger than ~ 0.3% (a typical value that has been widely used as a background level in air masses not impacted by active open biomass burning), the aerosol was generally regarded as the presence of BBOA. In this study, the f_{60} values in BBOA and agBBOA were 0.51% and 0.46%, respectively, demonstrating the presence of biomass burning related OA factors at WLG site.

In addition, biomass burning activeties in the QTP regions and its arrounding areas were quite common due to the widely usage of wood, grass, dung, and incense for residential cooking or worship at temple. More important, these biomass burning activeties occurred during all seasons rather than just winter or autumn seasons, so it was not strange to identify biomass burning related OA factors in summer season in the QTP regions.

The identification of the two types of BBOA in this study was not only based on the optimal selection of four-factor solution for PMF analysis, but also consist with the fact that biomass burning OAs would have different oxidation degrees when the emissions transported from surrounding areas to WLG site under different oxidation conditions and transport distances. Besides, similar OA source apportionment of two BBOA components with different oxidation degrees have also been resolved in previous studies, e.g., an additional oxygenated biomass-burning-influenced organic aerosol (OOA2-BBOA or OOA-BB) in the Paris metropolitan area (Crippa et al., 2013), urban Nanjing (Zhang et al., 2015) and Mt. Yulong (Zheng et al., 2017), respectively, besides the relatively fresh BBOA component.

Although the mass spectrum of agBBOA in this study looked like a semi-volatile OA, the time series of agBBOA was correlated tightly with $C_2H_4O_2^+$ (R^2 = 0.79). In addition, the mass spectrum of agBBOA was also resembled well with that of BBOA at QOMS (R^2 = 0.954). Therefore, on the basis of these evidences, the named oxygenated biomass-burning-influenced OA factor was reasonable in this study.

"Two biomass burning related OA factors, a relatively fresh biomass burning OA (BBOA) and an aged biomass burning OA (agBBOA), with distinctly different oxidation degrees were also found in this study. Although the *m/z* 44 signals were still the highest peaks for both the two factors, the *m/z* 60 signals, which were generally regarded as well-known tracers for biomass burning emissions (Alfarra et al., 2007), were also obvious in both HRMS. The fractions of the signals at *m/z* 60 (f_{60}) in their HRMS were 0.51 and 0.46%, respectively, which were significantly higher than the typical value of 0.3% that has been widely used as a background level in air masses not impacted by active open biomass burning in previous studies (Cubison et al., 2011; Zhou et al., 2017), demonstrating the presence of biomass burning related OA factors at WLG site. As shown in the Fig. 5, the time series of agBBOA correlated tightly with $C_2H_4O_2^+$ (R^2 = 0.79) and sulfate (R^2 = 0.47), while BBOA correlated slightly weak with $C_2H_4O_2^+$ (R^2 = 0.47) and potassium (R^2 = 0.30), respectively. The time series of agBBOA also correlated well with $C_xH_yO_1^+$ and $C_xH_yO_2^+$ ions, while BBOA correlated well with $C_xH_y^+$ and $C_xH_yO_1^+$ (Fig. S10). In addition, both the mass spectra of the two biomass burning related OA factors resembled well with that of BBOA at QOMS (R^2 of 0.886 and 0.954, respectively; Fig. S11; Zhang et al., 2018), whereas correlated moderately (R^2 = 0.39–0.59) with other standard BBOA mass spectra at other sites around the world (Aiken et al., 2009; Mohr et al., 2012). The agBBOA mass spectrum in this study correlated tightly (R^2 = 0.914) with the less oxidized oxygenated OA (LOOOA) identified at Nam Co station (Fig. S11; Xu et al., 2018). All these comparisons and correlation analysis further verified the reasonable source apportionment of OA in this study, namely there were two biomass burning related OAs at WLG, as a result of the different oxidation degrees of biomass burning emissions transported from surrounding areas to WLG site (see Sect. 3.4 for details). Similar OA source apportionment of two BBOA components with different oxidation degrees have also been resolved in previous studies, e.g., an additional oxygenated biomass-burning-influenced organic aerosol (OOA_2-BBOA or OOA-BB) in the Paris metropolitan area (Crippa et al., 2013), urban Nanjing (Zhang et al., 2015) and Mt. Yulong (Zheng et al., 2017), respectively, besides the relatively fresh BBOA component."

(3) The authors can also add, maybe to the supplement, more details on the way they selected the four factor solution, information about the Q/Qexp values, residuals, etc.

Thanks for the reviewer's insightful suggestion. We have added a key diagnostic plot to the supplement information, including the information about the Q/Q_{exp} as a function of factor number and *f*Peak, fractions of OA factors vs. *f*Peak, correlations among PMF factors, residuals or scaled residuals for each m/z and time, etc, which would help to understand the way we selected the four factor solution. The description of the figure is added in both the revised manuscript and supplement information, respectively.

"A summary of the key diagnostic plots of PMF results for this study is presented in Fig. S3. Overall, the PMF solutions were investigated from one to six factors with the rotational parameter (*f*Peak) varying from −1 to 1 with a step of 0.1. Finally, a four-factor solution with *f*Peak = 0 was

chosen in this study by examining the model residuals, scaled residuals and Q/Q_{exp} contributions for each m/z and time, as well as comparing the mass spectra of individual factor with reference spectra and the time series of individual factor with external tracers. The mass spectra, time series, and diurnal variations of PMF results from three-factor and five-factor solutions were also shown in Fig. S4 and S5 for comparison, respectively. The three-factor solution did not separate the two biomass burning factors whereas the five-factor solution showed a splitting factor."

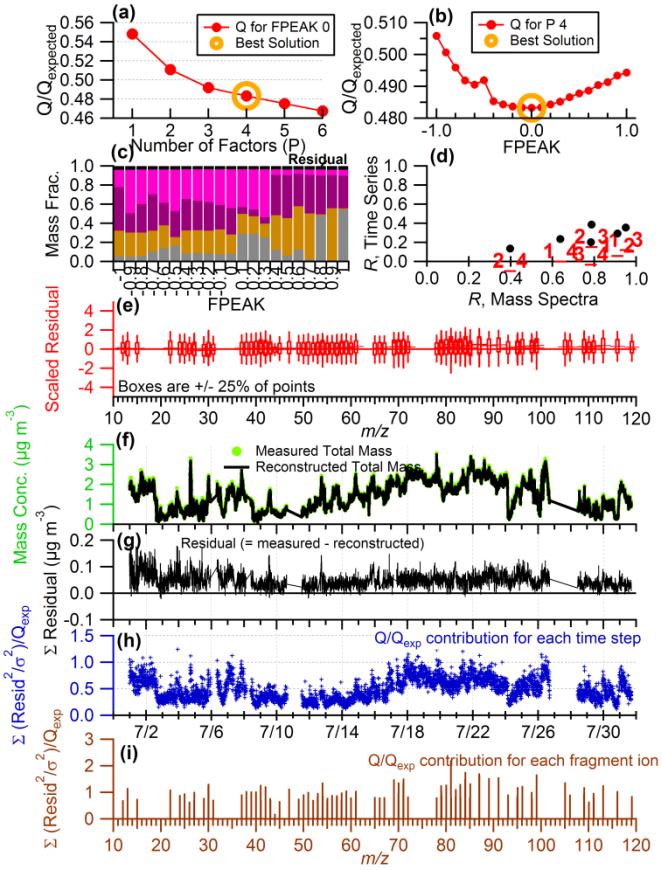

Figure S3. Summary of key diagnostic plots of the PMF results: **(a)** Q/Q_{exp} as a function of factor number (p) that selected for PMF analysis. For the best solution (four factors solution): **(b)** Q/Q_{exp} as a function of *f*Peak, **(c)** fractions of OA factors vs. *f*Peak, **(d)** correlations among PMF factors, **(e)** the box and whiskers plot showing the distributions of scaled residuals for each m/z, **(f)** time series of the measured organic mass and the reconstructed organic mass, **(g)** variations of the residual (= measured - reconstructed) of the fit, **(h)** the Q/Q_{exp} for each point in time, and **(i)** the Q/Q_{exp} values for each ion.

References

Aiken, A. C., DeCarlo, P. F., Kroll, J. H., Worsnop, D. R., Huffman, J. A., Docherty, K. S., Ulbrich, I. M., Mohr, C., Kimmel, J. R., Sueper, D., Sun, Y., Zhang, Q., Trimborn, A., Northway, M., Ziemann, P. J., Canagaratna, M. R., Onasch, T. B., Alfarra, M. R., Prevot, A. S. H., Dommen, J., Duplissy, J., Metzger, A., Baltensperger, U., and Jimenez, J. L.: O/C and OM/OC ratios of primary, secondary, and ambient organic aerosols with high-resolution time-of-flight aerosol mass spectrometry, Environ. Sci. Technol., 42, 4478-4485, doi:10.1021/es703009q, 2008.

Canagaratna, M. R., Jimenez, J. L., Kroll, J. H., Chen, Q., Kessler, S. H., Massoli, P., Hildebrandt Ruiz, L., Fortner, E., Williams, L. R., Wilson, K. R., Surratt, J. D., Donahue, N. M., Jayne, J. T., and Worsnop, D. R.: Elemental ratio measurements of organic compounds using aerosol mass spectrometry: characterization, improved calibration, and implications, Atmos. Chem. Phys., 15, 253-272, doi:10.5194/acp-15-253-2015, 2015.

Crippa, M., DeCarlo, P. F., Slowik, J. G., Mohr, C., Heringa, M. F., Chirico, R., Poulain, L., Freutel, F., Sciare, J., Cozic, J., Di Marco, C. F., Elsasser, M., Nicolas, J. B., Marchand, N., Abidi, E., Wiedensohler, A., Drewnick, F., Schneider, J., Borrmann, S., Nemitz, E., Zimmermann, R., Jaffrezo, J. L., Prévôt, A. S. H., and Baltensperger, U.: Wintertime aerosol chemical composition and source apportionment of the organic fraction in the metropolitan area of Paris, Atmos. Chem. Phys., 13, 961-981, doi:10.5194/acp-13-961-2013, 2013.

Cubison, M. J., Ortega, A. M., Hayes, P. L., Farmer, D. K., Day, D., Lechner, M. J., Brune, W. H., Apel, E., Diskin, G. S., Fisher, J. A., Fuelberg, H. E., Hecobian, A., Knapp, D. J., Mikoviny, T., Riemer, D., Sachse, G. W., Sessions, W., Weber, R. J., Weinheimer, A. J., Wisthaler, A., and Jimenez, J. L.: Effects of aging on organic aerosol from open biomass burning smoke in aircraft and laboratory studies, Atmos. Chem. Phys., 11, 12049-12064, doi:10.5194/acp-11-12049-2011, 2011.

Du, W., Sun, Y. L., Xu, Y. S., Jiang, Q., Wang, Q. Q., Yang, W., Wang, F., Bai, Z. P., Zhao, X. D., and Yang, Y. C.: Chemical characterization of submicron aerosol and particle growth events at a national background site (3295 m a.s.l.) on the Tibetan Plateau, Atmos. Chem. Phys., 15, 10811-10824, doi:10.5194/acp-15-10811-2015, 2015.

Wang, J., Zhang, Q., Chen, M., Collier, S., Zhou, S., Ge, X., Xu, J., Shi, J., Xie, C., Hu, J., Ge, S., Sun, Y., and Coe, H.: First Chemical Characterization of Refractory Black Carbon Aerosols and Associated Coatings over the Tibetan Plateau (4730 m a.s.l), Environ. Sci. Technol., 51, 14072-14082, doi:10.1021/acs.est.7b03973, 2017.

Xu, J., Zhang, Q., Chen, M., Ge, X., Ren, J., and Qin, D.: Chemical composition, sources, and processes of urban aerosols during summertime in northwest China: insights from high-resolution aerosol mass spectrometry, Atmos. Chem. Phys., 14, 12593-12611, doi:10.5194/acp-14-12593-2014, 2014.

Xu, J., Zhang, Q., Shi, J., Ge, X., Xie, C., Wang, J., Kang, S., Zhang, R., and Wang, Y.: Chemical characteristics of submicron particles at the central Tibetan Plateau: insights from aerosol mass spectrometry, Atmos. Chem. Phys., 18, 427-443, doi:10.5194/acp-18-427-2018, 2018.

Zhang, Q., Canagaratna, M. R., Jayne, J. T., Worsnop, D. R., and Jimenez, J. L.: Time- and size-resolved chemical composition of submicron particles in Pittsburgh: Implications for aerosol sources and processes, J. Geophys. Res., 110, D07S09, doi:10.1029/2004jd004649, 2005.

Zhang, X., Xu, J., Kang, S., Liu, Y., and Zhang, Q.: Chemical characterization of long-range transport biomass burning emissions to the Himalayas: insights from high-resolution aerosol mass spectrometry, Atmos. Chem. Phys., 18, 4617-4638, doi:10.5194/acp-18-4617-2018, 2018.

Zhang, Y. J., Tang, L. L., Wang, Z., Yu, H. X., Sun, Y. L., Liu, D., Qin, W., Canonaco, F., Prévôt, A. S. H., Zhang, H. L., and Zhou, H. C.: Insights into characteristics, sources, and evolution of submicron aerosols during harvest seasons in the Yangtze River delta region, China, Atmos. Chem. Phys., 15, 1331-1349, doi:10.5194/acp-15-1331-2015, 2015.

Zheng, J., Hu, M., Du, Z., Shang, D., Gong, Z., Qin, Y., Fang, J., Gu, F., Li, M., Peng, J., Li, J., Zhang, Y., Huang, X., He, L., Wu, Y., and Guo, S.: Influence of biomass burning from South Asia at a high-altitude mountain receptor site in China, Atmos. Chem. Phys., 17, 6853-6864, doi:10.5194/acp-17-6853-2017, 2017.

Zhou, S., Collier, S., Jaffe, D. A., Briggs, N. L., Hee, J., Sedlacek Iii, A. J., Kleinman, L., Onasch, T. B., and Zhang, Q.: Regional influence of wildfires on aerosol chemistry in the western US and insights into atmospheric aging of biomass burning organic aerosol, Atmos. Chem. Phys., 17, 2477–2493, https://doi.org/10.5194/acp-17-2477-2017, 2017.

Chemical characterization and sources of submicron aerosols in the northeastern Qinghai-Tibet Plateau: insights from high-resolution mass spectrometry

Xinghua Zhang[1,2,3], Jianzhong Xu[1], Shichang Kang[1], Qi Zhang[4], Junying Sun[5]

[1]State Key Laboratory of Cryospheric Sciences, Northwest Institute of Eco-Environment and Resources, Chinese Academy of Sciences, Lanzhou 730000, China
[2]Key Laboratory of Arid Climatic Change and Reducing Disaster of Gansu Province, Key Laboratory of Arid Climatic Change and Disaster Reduction of CMA, Institute of Arid Meteorology, China Meteorological Administration, Lanzhou 730020, China
[3]University of Chinese Academy of Sciences, Beijing 100049, China
[4]Department of Environmental Toxicology, University of California, Davis, CA 95616, USA
[5]Chinese Academy of Meteorological Sciences, China Meteorological Administration, Beijing 100081, China

Correspondence to: Jianzhong Xu (jzxu@lzb.ac.cn)

Abstract

An Aerodyne high-resolution time-of-flight aerosol mass spectrometer (HR-ToF-AMS) was deployed along with other online instruments to study the highly time-resolved chemistry and sources of submicron aerosols (PM_1) at Waliguan (WLG) Baseline Observatory, a high-altitude (3816 m a.s.l.) background station located at the northeast~~ern~~ edge of Qinghai-Tibet Plateau (QTP), during 1−31 July 2017. The average PM_1 mass concentration during this study was 9.1 μg m^{-3} (ranging from 0.3 to 28.1 μg m^{-3}), which was distinctly higher than those (2.0–5.7 μg m^{-3}) measured with Aerodyne AMS at other high-elevation sites in the southern or central QTP. Sulfate showed dominant contribution (38.1%) to PM_1 at WLG following by organics (34.5%), ammonium (15.2%), nitrate (8.1%), BC (3.0%) and chloride (1.1%). Accordingly, bulk aerosols appeared to be slightly acidic throughout this study mainly related to the enhanced sulfate contribution. All chemical species peaked at the accumulation mode, indicating the well mixed and highly aged aerosol particles at WLG from long-range transport. Positive matrix factorization (PMF) on the high-resolution organic mass spectra resolved four distinct organic aerosol (OA) components, including a traffic-related hydrocarbon-like OA (HOA), a relatively fresh biomass burning OA (BBOA), an aged biomass burning OA (agBBOA) and a more-oxidized oxygenated OA (OOA). On average, the two relatively oxidized OAs, OOA and agBBOA, contributed 34.4% and 40.4% of organics, respectively, while the rest were 18.4% for BBOA and 6.8% for HOA. Source analysis for air masses displayed that higher mass concentrations of PM_1 and enhanced contributions of sulfate and biomass burning related OA components (agBBOA + BBOA) were from northeast of the WLG with shorter transport distance, whereas lower PM_1 mass concentrations with enhanced OOA contribution were from west after long-range transport, suggesting their distinct aerosol sources and significant impacts of regional transport ~~to~~ on aerosol mass loadings and chemistry at WLG.

1 Introduction

The Qinghai-Tibet Plateau (QTP) is one of the most remote and pristine region in the world. Its huge surface area (~ 2,500,000 km^2) and high elevation (with a mean elevation of more than 4000 m above sea level (a.s.l.)) make it especially important in earth sciences and therefore the QTP is generally called as the "third pole" (Yao et al., 2012). According to its high elevation, sparse population and minor local anthropogenic activities, the QTP is regarded as an ideal area for observing the natural background aerosol and long-range transported aerosol. In recent decades, a certain number of studies have presented convincing evidence for the long-range transport of air pollutants from the surrounding areas to the QTP (Engling et al., 2011; Xia et al., 2011; Lüthi et al., 2015; Zhang et al., 2017). Particularly, air pollutants from the southern and southeastern Asia, two of the major regions with enhanced biomass burning emissions in the world, would stack up in the southern foothills of the Himalayas during the pre-monsoon season, then climbed over Himalayas by the topographic lifting and the mountain-valley breeze circulation, and finally moved upward to QTP (Lüthi et al., 2015). These long-range transport following by deposition of polluted air masses, especially for the two important light-absorbing substances of black carbon (BC) and brown carbon (BrC), have significant impacts on climate, environment and hydrology in the QTP (Xu et al., 2009; Kang et al., 2010; Qian et al., 2011; Yang et al., 2014).

In contrast, aerosol particles in the northern QTP showed quite different behaviors comparing with ~~that~~ those in the southern QTP due to the different aerosol sources and climate for these two regions. For example, Li et al. (2016) found equal important contributions from fossil fuel (46%) and biomass (54%) aerosol sources to BC in the Himalayas, nevertheless~~however~~, it was dominated by fossil fuel combustion (66%) in the northern QTP. Correspondingly, the chemical composition of ambient aerosol in the northern QTP was also distinctly different with that in the southern QTP. Xu et al. (2014a, 2015) conducted aerosol compositions studies from filter measurements of $PM_{2.5}$ (particulate matter with diameter less than 2.5 μm) at the Qilian Shan Station observatory at the northeast edge of QTP, and found sulfate was ~~a~~ the dominant component during summer season due to the influence of anthropogenic emissions from industrial areas in the northwestern China~~inland of northwest China~~. Similar results were also found ~~in~~ by Li et al. (2013) and Zhang et al. (2014) which conducted field studies in the northeast~~ern~~ part of QTP. Nitrate, oxidized from the nitric oxides (NO_x), was also an important component in the northern QTP which could interact with mineral dust during transport (Xu et al., 2014a). Due to the relatively lower elevation comparing with the southern QTP (< 4000 vs. > 5000 m a.s.l.), the polluted air masses are easily transported to the mountain areas in the northern QTP forced by the strong~~ly~~ mountain-valley breeze during summer (Xu et al., 2013). Besides the significant impacts by anthropogenic emissions from the northwestern China or Indian subcontinent, air pollutants to the northeastern QTP could also from the central Eurasian continent (Xue et al., 2013).~~In addition, air pollutants to the northern QTP could also from the central Eurasian continent where locates in the upstream of the northwest of China, although relatively lower air masses presented comparing with those impacted by anthropogenic emissions from China and the Indian subcontinent (Xue et al., 2013).~~ However, most of the previous studies ~~in the northeastern QTP~~ for characterizing the chemical properties and sources of aerosol particles in the northeastern QTP were heavily based on the filter or snow/ice samples with low time resolution ranging from days to weeks, mainly

because of the absent deployment of real-time instruments at the remote region with harsh environments, challenging weather conditions and logistical difficulties. Studies focused on the atmospheric aerosol chemical compositions in the northeastern QTP using the high-time-resolution real-time measurements are still relatively rare until now.~~The real-time measurement of atmospheric aerosol chemistry with high time resolution is still relatively rare in the northern QTP until now.~~

The Aerodyne aerosol mass spectrometer (AMS) is a~~n~~ unique instrument which can provide ~~both~~ chemical composition and/or size distribution information of non-refractory submicron aerosol ($NR\text{-}PM_1$) ~~species~~ with high time resolution and sensitivity (Jayne et al., 2000; Jimenez et al., 2003; Canagaratna et al., 2007). AMS has been widely implemented worldwide in recent decades, especially in China since 2006 due to the great concern of~~high attention to~~ atmospheric environment (Li et al., 2017, and references therein). Besides the typical applications for studying air pollution in these urban/rural sites, e.g. megacities with severe haze pollution in eastern China, AMS has also been successfully deployed at many remote sites ~~in China~~ due to its low detection limit~~ation~~ (see details in Table 1 of Xu et al. (2018) and Table S1 of Zhang et al. (2018)). In recent years, the deployments of AMS in the highland areas of QTP have been conducted in ~~various~~ a few field studies (Fig. S1), including a high-resolution time-of-flight AMS (HR-ToF-AMS) and a soot particle AMS (SP-AMS) at Nam Co in the central QTP (Wang et al., 2017; Xu et al., 2018), a HR-ToF-AMS at QOMS in the southern QTP (Zhang et al., 2018) and a HR-ToF-AMS at Mt. Yulong in the southeastern QTP (Zheng et al., 2017)~~ in the southern QTP, and an Aerodyne aerosol chemical speciation monitor (ACSM) at Menyuan in the northeastern QTP (Du et al., 2015)~~. ~~Consistent with those filter samplings, the dominant contributions of organics (54−68%) but low PM_1 ($NR\text{-}PM_1$ + BC) mass loadings (2.0−5.7 μg m^{-3}) were all found in those AMS studies conducted in the southern or central QTP (Zheng et al., 2017; Xu et al., 2018; Zhang et al., 2018), mainly associated with the significant impacts of long-range transport biomass burning emissions from southern Asia, whereas relatively few studies were conducted in the northern QTP.~~In addition to the low PM_1 ($NR\text{-}PM_1$ + BC) mass loadings, the dominant contribution from organic aerosol (OA) (54−68%) was found in the southern and central QTP (Zheng et al., 2017; Xu et al., 2018; Zhang et al., 2018). OA was composed by oxygenated OA (OOA) and biomass burning related OA (BBOA) components in those high-altitude background sites. The OOA component was associated with the intense oxidation processes that converted the fresh OA to secondary OA, while BBOA was related to the direct emissions from the biomass burning activities in the highland areas. However, relatively few studies have been conducted in the northern QTP except a measurement using Aerodyne aerosol chemical speciation monitor (ACSM) at Menyuan (Du et al., 2015).

In this study, a HR-ToF-AMS with other real-time collocated instruments were first deployed at the Waliguan (WLG) Baseline Observatory, which was one of the World Meteorological Organization's (WMO) Global Atmospheric Watch (GAW) baseline observatories, located in the northeastern QTP, to characterize the submicron aerosol chemical compositions and sources during summer season. The ~~5-min~~ real-time characterizations of submicron aerosols including mass concentrations, chemical composition, size distribution as well as temporal and diurnal variations were presented in details in this study. Source apportionment using positive matrix

factorization (PMF) analysis on the high-resolution OA mass spectrum ~~of organic aerosol (OA)~~ was conducted to investigate the sources and chemical evolution of OA during long-range transport. Finally, back trajectories of air masses were then performed to present the possible sources and pathway of ambient aerosols during the sampling period.

2 Experimental methods

2.1 Site and measurements

The field study was carried out during 1−31 July 2017 within the typical warm and rainy season at the Waliguan (WLG) Baseline Observatory (36°17′ N, 100°54′ E, 3816 m a.s.l.), which ~~locates in~~ is located at the top of Mt. Waliguan at the northeast~~ern~~ edge of QTP in western China with an ~ 600 m elevation difference from the surrounding ground (Fig. 1a and b). Mt. Waliguan is a relatively remote area and generally covered by typical highland vegetation, e.g., highland grassland and tundra, and constructed as an in-land baseline station of Global Atmosphere Watch (GAW) since 1994 (http://www.wmo.int/pages/prog/arep/gaw/gaw_home_en.html). The closest town, ~~GongHe~~ Gonghe County, is located ~ 30 km to the west of Mt. Waliguan and with a population of ~ 30,000, while Xining, the capital city of Qinghai ~~Province~~province, China, is the closest concentrated population center located about 90 km to the northeast and with a population of 2.35 millions. A national road is about 9 km to the north of Mt. Waliguan, yet with relative light vehicle traffic. Therefore, there are no strong anthropogenic source emissions around Mt. Waliguan. The date and time used in this study are reported in local time, i.e., Beijing Time (BJT: UTC + 8 h).

2.2 Instrumentation

Aerosol ~~particle~~ measurements were performed at the top floor of the main two-story building at WLG observatory from 1 to 31 July 2017 with a suit of real-time instruments, including a HR-ToF-AMS (Aerodyne Research Inc., Billerica, MA, USA) for ~~5 min~~ size-resolved chemical compositions (organics, sulfate, nitrate, ammonium and chloride) of NR-PM_1, a photoacoustic extinctiometer (PAX, DMT Inc., Boulder, CO, USA) for particle light absorption and scattering coefficients (b_{abs} and b_{scat}) at 405 nm and the black carbon (BC) mass concentration through a constant mass absorption efficient (MAE) value of 10.18 m^2 g^{-1}, and a cloud condensation nuclei counter (CCN-100, DMT Inc., Boulder, CO, USA) for the number concentration of cloud condensation nuclei (CCN) that can form into cloud droplets. Simultaneously, other synchronous data were also acquired at the WLG baseline observatory during the sampling period, including the mass concentrations of $PM_{2.5}$ and PM_{10} (particulate matter with diameter less than 10 μm) measured by a TEOM 1405-DF dichotomous ambient particulate monitor with a filter dynamics measurement system (Thermo Scientific, Franklin, MA, USA) and gaseous pollutants of carbon monoxide (CO) and ozone (O_3) measured using the Thermo gas analyzers (Model 48i and 49i, respectively, Thermo Scientific, Franklin, MA, USA). The setup of instruments in this study was shown in Fig. 1d. Ambient particles were sampled through an inlet system, including a $PM_{2.5}$ cyclone (model URG-2000-30EH, URG Corp., Chapel Hill, NC, USA) for removing coarse particles with size cutoffs of 2.5 μm, a nafion dryer following the cyclone to dry the ambient air

and eliminate the potential humidity effect on particles, and 0.5 inch stainless steel tubes. The inlet stepped out of the building rooftop about 1.5 m, and the total air flow of the inlet was about 12.5 L min^{-1}, maintained by a vacuum pump with a flow rate of 10 L min^{-1} for the $PM_{2.5}$ size cut, and the other part of flow rate by the instruments. The room temperature was maintained at ~ 18 °C by two air conditioners. In addition, a Vantage Pro2 weather station (Davis Instruments Corp., Hayward, CA, USA) was set up on the building rooftop to obtain the real-time meteorology data, including ambient temperature (*T*), relative humidity (RH), wind speed (WS), wind direction (WD), solar radiation (SR), and precipitation (Precip.).

The details of the Aerodyne HR-ToF-AMS has been described elsewhere (DeCarlo et al., 2006). Briefly, a 120 μm critical orifice (replaced the typical 100 μm for enhancing the transmission efficiency at high-altitude area) and an aerodynamic lens were settled in the front inlet system to sample and focus the ambient particles into a concentrated and narrow beam. The focused particle beam exiting the lens was accelerated into the particle-sizing vacuum chamber to obtain the aerodynamic size of particles by a rotating wheel chopper. Then, particles were vaporized thermally at ~ 600 °C by a resistively heated surface and ionized by a 70 eV electron impact, and finally, detected by a high-resolution mass spectrometer. The chopper generally worked at three positions alternately, i.e., open, close, and chopping positions, for measuring the bulk and background signals as well as the size-resolved spectral signals of airborne particles, respectively. Similar to most of the previous AMS field measurements~~In this study~~, the mass spectrometer was toggled under the high sensitive V-mode (detection limits ~ 10 ng m^{-3}) and the high resolution W-mode (~ 6000 m/Δm) every 5 min in this study. Under the V-mode operation, the instrument also switched between the mass spectrum (MS) mode and the particle P-ToF mode every 15 s to obtain the mass concentrations and size distributions of NR-PM_1 species, respectively, whereas the high resolution W-mode was used to obtain high resolution mass spectral data. However, ~~Note that~~ the data and error matrices ~~input~~inputted into the PMF analysis were finally generated from ~~analyzing~~ the V-mode data ~~via PIKA fitting~~ rather than the W-mode data in this study due to the low aerosol mass loading at WLG. Hence, all the data used in this study are from V-mode with 10 min time resolution.

2.3 Data processing

The HR-ToF-AMS data were processed using the standard AMS analysis software of SQUIRREL (v1.56) to determine the mass concentrations and size distributions of NR-PM_1 species and the high resolution data analysis software of PIKA (v1.15c) to analyze the ion-speciated mass spectra, components and elemental compositions (e.g., oxygen-to-carbon (O/C), hydrogen-to-carbon (H/C), nitrogen-to-carbon (N/C) and organic mass-to-organic carbon (OM/OC) ratios using the "improved-ambient" method (Canagaratna et al., 2015)) of organics in this study. A collection efficiency (CE) was introduced to compensate for the incomplete transmission and detection of particles due to particle bouncing at the vaporizer and partial transmission through the aerodynamic lens. Middlebrook et al. (2012) had evaluated the dependency of CE on several ambient properties and concluded a composition-dependent CE parameterization according to the sampling line RH, aerosol acidity, and mass fraction of ammonium nitrate (ANMF). High RH, high aerosol acidity or high ANMF values would all increase the CE obviously. However, in this

study, (1) aerosol particles were dried totally through a nafion dryer in the inlet system and made sure that RH in the sampling line were below 40%; (2) aerosol particles were just slightly acidic as indicated by the average ratio (0.86) of measured ammonium to predicted ammonium (see Sect. 3.1 and Fig. 3a for details); (3) ANMF values were normally below 0.4 during the entire sampling period as shown in Fig. ~~S1~~S2. Therefore, these three parameters were all expected to have negligible effects on the quantification of aerosol species from our AMS data set and thus a constant CE of 0.5, which has been widely used in previous field AMS studies, was finally employed in this study.

The source apportionment of organics in this study was conducted by ~~Positive matrix factorization (~~PMF~~)~~ analysis using the PMF2.exe algorithm (v4.2) (Paatero and Tapper, 1994) and PMF Evaluation Tool (PET, v2.03) (Ulbrich et al., 2009) in robust mode on the high resolution organic mass spectrum. ~~Note that the data and error matrices input into the PMF analysis were generated from analyzing the V-mode data via PIKA fitting rather than W-mode in this study due to the low aerosol mass loading at WLG.~~ The PMF analysis was thoroughly evaluated following the procedures summarized in Table 1 of Zhang et al. (2011), including modifying the error matrix, down-weighting or removing the low signal-to-noise (*S*/*N*) ions, etc. For example, the signals of H_2O^+ and CO^+ for organics were scaled to that of CO_2^+ ~~during this study~~ as $CO^+ = CO_2^+$ and $H_2O^+ = 0.225 \times CO_2^+$ ~~according to Aiken et al. (2008)~~, while signals of HO^+ and O^+ were set as $HO^+ = $ ~~0.23~~0.25 $\times H_2O^+$ and $O^+ = 0.04 \times H_2O^+$ according to Aiken et al. (2008)~~based on the fragmentation pattern of water molecules (Xu et al., 2014b), respectively~~. Then the above four ions were further down-weighted by increasing their errors by a factor of 2 in PMF analysis. Isotopic ions were generally excluded because their signals are not directly measured. The "bad" ions with $S/N < 0.2$ were removed from the data and error matrices, while the "weak" ions with $0.2 < S/N < 2$ were downweighted by increasing their errors. In addition, some runs with huge residual spikes, e.g., data with much too low mass loadings related with the heavy rain on 27 July 2017, were also removed from the data and error matrices. A summary of the key diagnostic plots of PMF results for this study is presented in Fig. S3. Overall, the PMF solutions were investigated from one to six factors with the rotational parameter (*f*Peak) varying from −1 to 1 with a step of 0.1. Finally, a four-factor solution with *f*Peak = 0 was chosen in this study by examining the model residuals, scaled residuals and Q/Q_{exp} contributions for each *m*/*z* and time, as well as comparing the mass spectra of individual factor with reference spectra and the time series of individual factor with external tracers. The mass spectra, time series, and diurnal variations of PMF results from three-factor and five-factor solutions were also shown in Fig. ~~S2~~ S4 and ~~S3~~ S5 for comparison, respectively. The three-factor solution did not separate the two biomass burning factors whereas the five-factor solution showed a splitting factor.

3 Results and discussion

3.1 Size-resolved chemical characteristics of PM_1

An overview of temporal variations of mass concentrations and fractions of PM_1 chemical species (organics, sulfate, nitrate, ammonium, chloride and BC) as well as meteorological conditions (*T*, RH, WS, WD, and Precip.), mass concentrations of relevant particulate matters ($PM_{2.5}$ and PM_{10}) and gaseous pollutants (O_3 and CO), and mass fractions of organic components are shown in Fig.

2, respectively. The m~~M~~issing data are due to hardware or software malfunction, maintenance of the instrument, or removing large spikes and unique burning event (a local Tibetan festival event occurred during 5−6 July 2017 with extremely high aerosol mass loadings) in data processing. Air temperature (T) ranged from 8.5 to 14.5 °C for the averaged diurnal variation during the study, with an average (± 1σ) of 11.0 ± 2.0 °C, while relative humidity (RH) ranged from 55.9 to 73.5% with an average of 66.6 ± 5.7% (Fig. ~~S4~~S6). The wind directions (WD) at WLG were predominantly by eastern, southeastern and northeastern during this study, with an average wind speed (WS) of 4.4 ± 2.8 m s^{-1} (Fig. 1c and 2b). In addition, WD generally changed from eastern to southeastern during the nighttime with WS higher than 4 m s^{-1}, whereas from northwestern to northeastern during the daytime with relatively lower WS (Fig. ~~S4~~S6). Two moderate rain events occurred during 2−9 and 22−28 July 2017, with daily mean precipitation~~values~~ of 2.6 and 7.4 mm d^{-}~~^{3}~~1, respectively (Fig. 2a).

The total PM_1 mass varied dynamically throughout this study with ~~5-min~~ mass concentration ranging from 0.3 to 28.1 μg m^{-3}. This dynamic variation pattern could also be found for the mass concentrations of $PM_{2.5}$, PM_{10} and CO, with their correlation coefficients (R^2) versus PM_1 varying reasonably from 0.39 to 0.63 (Fig. 2 and ~~S4~~S7). In addition, PM_1 accounted 66% of $PM_{2.5}$ mass in this study (Fig. ~~S5~~S7), reflecting essentially contribution of submicron aerosols at WLG. Overall, the average mass concentration of total PM_1 (± 1σ) at WLG for the entire study was 9.1 (± 5.3) μg m^{-3}, which was much higher than those at other high-elevation sites in the QTP measured with Aerodyne AMS, such as 2.0 μg m^{-3} between 31 May and 1 July 2015 at Nam Co Station (4730 m a.s.l.) in the central ~~of~~ QTP (Xu et al., 2018), 4.4 μg m^{-3} between 12 April and 12 May 2016 at QOMS (4276 m a.s.l.) at the south~~ern~~ edge of QTP (Zhang et al., 2018), and 5.7 μg m^{-3} between 22 March and 14 April 2015 at Mt. Yulong (3410 m a.s.l.) at the southeastern ~~edge of~~ QTP (Zheng et al., 2017), whereas this value was comparable with that (11.4 μg m^{-3}) measured with an Aerodyne ACSM between 5 September and 15 October 2013 at Menyuan (3295 m a.s.l.) at the northeastern QTP (Du et al., 2015). The high~~er~~ PM_1 mass concentration at WLG in the northeastern QTP comparing with those at other sites in the central or southern QTP was likely due to the relatively shorter distance from the ~~polluted city center~~industrial areas (e.g., Xining city) in the northwestern China and strong~~ly~~ mountain-valley breeze during summer. This conclusion could be supported by the comparisons of air mass back-trajectories between WLG in this study (see Sect. 3.4 for details) and those at Nam Co Station in Xu et al. (2018) and QOMS in Zhang et al. (2018). Sulfate and organics were the two dominant PM_1 species at WLG, accounting for 38.1% and 34.5% on average, respectively, followed by ammonium (15.2%), nitrate (8.1%), BC (3.0%) and chloride (1.1%). This chemical composition of PM_1 at WLG was quite different with those at Nam Co, QOMS and Mt. Yulong sites in the central or southern QTP (Zheng et al., 2017; Xu et al., 2018; Zhang et al., 2018), where organics was the dominant species accounting for 54−68% of total PM_1 mass due to the significant contribution of biomass burning emissions, whereas sulfate only contributed 9−15% of total PM_1. The consistent high contribution of sulfate was also observed at Menyuan (28%) in the northeastern QTP and other rural and remote sites (19−64%) in East Asia which were far away from urban areas, as that summarized in Fig. 1 in Du et al. (2015). Moreover, as displayed in Fig. 3b, mass contribution of sulfate increased significantly with the increase of total PM_1 mass (lower than 15% for PM_1 mass equal to 1.0 μg m^{-3} and increased to

more than 45% for PM_1 mass of 20.0 μg m^{-3}), suggesting important contribution of sulfate to submicron aerosols at WLG.

Bulk acidity of PM_1 at WLG was also evaluated according to the method in Zhang et al. (2007)~~,~~ ~~namely using the ratio of measured ammonium to~~. ~~the~~ The predicted ammonium ~~that~~ was calculated based on the mass concentrations of sulfate, nitrate and chloride and assumed full neutralization of these anions by ammonium. The PM_1 appeared to be slightly acidic throughout this study, as indicated by the scatter plot between the measured and predicted ammonium in Fig. 3a (Slope = 0.86, R^2 = 0.98). The acidic feature of aerosol particles at WLG was consistent with those results at Menyuan (Du et al., 2015) and Qilian Shan Mountain (Xu et al., 2015) that both located in the northeastern QTP, but different with those at Nam Co (Xu et al., 2018) and QOMS (Zhang et al., 2018) in the central or southern ~~edge of~~ QTP where bulk aerosol particles were generally neutralized or excesses of ammonium. The enriched sulfate in the northeastern QTP might be related tightly with the enhanced coal consumption in the northwest of China and aqueous processing by cloud at the mountains. This conclusion could be further demonstrated by the emission distribution of sulfur dioxide (SO_2) in China observed by the Ozone Monitoring Instrument (OMI) satellite ~~instrument~~ data in previous studies (Lu et al., 2011; van der A et al., 2017), where SO_2 showed considerable concentrations in the northwest of China, especially in urban areas like Xining and Lanzhou cities, whereas extremely low concentrations occurred in the southern QTP.

The average chemically-resolved size distributions of mass concentrations of NR-PM_1 species are shown in Fig. 3c. Overall, all chemical species peaked at the accumulation mode with different peaking sizes, e.g. ~ 400 nm in aerodynamic diameter (D_{va}) for organics, ~ 450 nm for chloride, and ~ 500 nm for the rest three secondary inorganic species (sulfate, nitrate and ammonium), indicating the well mixed and highly aged aerosol particles at WLG during the sampling period. Moreover, organics presented relatively wider distribution than the three secondary inorganic species in the small sizes (< 300 nm). This could also be clearly revealed by the variations of mass contribution of chemical species as a function of particle sizes in Fig. 3d. The contribution of organics decreased apparently with the increasing sizes whereas those of three inorganic species, especially sulfate, increased correspondingly. Specifically, organics could contribute~~d~~ more than half of the ultrafine NR-PM_1 (D_{va} < 100 nm) that maybe associated with the existing of relatively fresh sources of organic particles, while the three inorganic species dominated (more than 60%) at the accumulation mode due to their highly aged properties.

3.2 Bulk characteristics and elemental composition of OA

The average high-resolution mass spectrum (HRMS) and elemental compositions of OA during the study were shown in Fig. 4a. Note that the elemental ratios of O/C, H/C, N/C and OM/OC in this study were all determined using the "improved-ambient" method (Canagaratna et al., 2015), which increased O/C by 29%, H/C by 14% and OM/OC by 15% on average, respectively, comparing with those determined from the "Aiken ambient" method (Aiken et al., 2008) (Fig. ~~S6~~S8). The average HRMS of OA was quite similar with those at other locations, e.g., Menyuan (Du et al., 2015), Nam Co (Xu et al., 2018) and QOMS (Zhang et al., 2018) in the QTP, with

significantly high contribution at *m/z* 44 (17.9%; composed totally by CO_2^+ in this study and similarly hereinafter; ~~17.9%~~). On average, $C_xH_yO_1^+$ dominated the total OA (44.0%) followed by $C_xH_y^+$ (27.9%), $C_xH_yO_2^+$ (21.7%), $H_yO_1^+$ (5.1%), $C_xH_yN_p^+$ (1.0%) and $C_xH_yO_zN_p^+$ (0.2%), as shown in pie chart in Fig. 4a. The total contributions of the two major oxygenated ion fragments ($C_xH_yO_z^+$) was 65.7% at WLG, which was comparable to those values at Nam Co during 31 May–1 July 2015 (57.9%; Xu et al., 2018) and QOMS during 12 April–12 May 2016 (66.2%; Zhang et al., 2018), whereas much higher than that (38.0%) measured during 11 July–7 August 2012 at Lanzhou~~, an urban city located at the northeastern edge of QTP~~ (Xu et al., 2014b). In addition, the average O/C ratio of 0.99 in this study was also comparable with those at Nam Co (0.88; determined by "improved-ambient" method and similarly hereinafter; Xu et al., 2018) and QOMS (1.07; Zhang et al., 2018), but quite higher than those observed at various urban and rural sites in China during summertime, e.g., 0.53 and 0.56 in Beijing, 0.40 in Shanghai, 0.41 in Shenzhen and 0.36 in Jiaxing (Hu et al., 2017). As either the contributions of CO_2^+ and $C_xH_yO_z^+$ or element ratio of O/C are generally considered as good indicators for the aging degree of OA, the relatively higher values at WLG as well as at other sites in the QTP together indicated that OA in the QTP was highly oxidized due to the absence of local emissions and long-range transport.

Diurnal cycles of O/C and OM/OC ratios in this study varied shallowly within 0.96−1.05 and 2.40−2.52, respectively, suggesting an overall OA source from regional transport ~~organic aerosol source~~ at WLG (Fig. 4b). ~~The relatively higher values during afternoon (16:00−17:00 BJT) but lower values during morning (9:00−10:00 BJT) were mainly related to the different aerosol sources and photochemical oxidation conditions during long-range transport. Besides, the ratios of O/C and OM/OC were relatively stable and even higher during nighttime than those in the morning, which may be induced by the consistent OA source from long-range transport at night whereas relatively fresh OA enhanced in the morning.~~ The relatively higher O/C and OM/OC during afternoon potentially related with the photochemical oxidation processes in the daytime, while lower values in the late morning mainly associated with the transport of relatively fresh OA from nearby areas to WLG site, which could be further revealed by the corresponding higher H/C and N/C ratios in the late morning as well as the diurnal variations of the two primary OA components (see Sect. 3.3 for details). Correspondingly, the H/C ratio presented an opposite diurnal pattern comparing with O/C. The elemental ratios in the Van Krevelen diagram (H/C versus O/C), which had been used widely to probe the oxidation reaction mechanisms for bulk OA, were calculated following a slope of –0.64 in this study (Fig. ~~S6~~S8), which suggested that the OA oxidation mechanism at WLG was a combination of carboxylic acid groups with fragmentation and alcohol/peroxide functional groups without fragmentation (Heald et al., 2010).

3.3 Source apportionment of OA

PMF analysis on the OA HRMS ~~of OA~~ identified four distinct components, i.e., a traffic-related hydrocarbon-like OA (HOA), a relatively fresh biomass burning OA (BBOA), an aged biomass burning OA (agBBOA) and a more-oxidized oxygenated OA (OOA) in this study. Each of OA components had unique characteristics on mass spectral profile, average element ratios, diurnal pattern, and temporary variation as well as tight correlations with corresponding tracers. The details on the source apportionment results of OA are given as follows.

Figure 5 shows the average HRMS and temporal variation of each OA component, respectively. A traffic-related hydrocarbon-like OA (HOA), with the lowest O/C ratio (0.33) and the highest H/C ratio (1.83) among the four factors, was identified in this study. Similar to several HOA mass spectra reported in previous studies (Zhang et al., 2005; Ng et al., 2011), HRMS of HOA in this study was also dominated by hydrocarbon ion series of $C_nH_{2n\pm1}^+$, especially $C_3H_5^+$ (m/z = 41), $C_3H_7^+$ (m/z = 43), $C_4H_7^+$ (m/z = 55), $C_4H_9^+$ (m/z = 57), $C_5H_9^+$ (m/z = 69), and $C_5H_{11}^+$ (m/z = 71), as shown in Fig. 5a. Consequently, the dominant contribution of ion fragment was $C_xH_y^+$ (62.8%) follow by $C_xH_yO_1^+$ (29.3%) and $C_xH_yO_2^+$ (6.1%) (Fig. ~~S7~~S9), suggesting the primary feature of HOA compared with other OA components. The two dominant ions, m/z 57 (mainly $C_4H_9^+$ and $C_3H_5O^+$) and m/z 55 (mainly $C_4H_7^+$ and $C_3H_3O^+$), which are generally associated with primary organics from combustion sources, are commonly considered as tracers for HOA in previous studies (Zhang et al., 2005). In our study, HOA contributed 71 and 27% to $C_4H_7^+$ and $C_3H_3O^+$, respectively, at m/z 55 while 89 and 29% to $C_4H_9^+$ and $C_3H_5O^+$ at m/z 57. The time series of HOA correlated closely with those of $C_4H_9^+$ (R^2 = 0.68, Fig. 5e) and other alkyl fragments, like $C_3H_7^+$, $C_4H_7^+$, $C_5H_9^+$ (R^2 = 0.52−0.65, Fig. ~~S8~~S10). Besides, the high-resolution mass spectrum of HOA was highly similar to those from other locations around the world (Aiken et al., 2009; Elser et al., 2016; Hu et al., 2016), with correlation coefficients (R^2) varying from 0.62 to 0.94 (Fig. ~~S9~~S11). Diurnal variation of HOA (Fig. 6c and d) in this study presented two slight peaks in the late morning (around 10:00 BJT) and evening (around 20:00 BJT), respectively. Although there was not traffic rush hour in the high-elevation site, the increasing vehicles on the national road combined with the valley breeze together lead to the slightly higher HOA concentrations in the late morning, then HOA decreased continuously with the increasing planetary boundary layer (PBL) height in the afternoon and elevated again to a stable high level during the nighttime due to the low PBL height and mountain breeze. Note that the O/C ratio of HOA in this study was obviously higher than those (generally lower than 0.2) observed in either urban sites or laboratory studies where have intense local traffic emissions (He et al., 2010; Sun et al., 2011; Xu et al., 2016). The reason is mainly due to the regional transport of traffic emission to WLG. As mentioned in Sect. 2.1, one national road is about 9 km to the north of Mt. Waliguan yet with relative light vehicle traffic. Hence, the traffic related aerosols from either the national road or nearby towns and cities would undergo certain oxidation processes during transportation to WLG site.

Two biomass burning related OA factors, a relatively fresh biomass burning OA (BBOA) and an aged biomass burning OA (agBBOA), with distinctly different oxidation degrees were also found in this study. Although the m/z 44 signals were still the highest peaks for both the two factors, the m/z 60 signals, which were generally regarded as well-known tracers for biomass burning emissions (Alfarra et al., 2007), were also obvious in both HRMS. The fractions of the signals at m/z 60 (f_{60}) in their HRMS were 0.51 and 0.46%, respectively, which were significantly higher than the typical value of 0.3% that has been widely used as a background level in air masses not impacted by active open biomass burning in previous studies (Cubison et al., 2011; Zhou et al., 2017), demonstrating the presence of biomass burning related OA factors at WLG site. ~~The O/C and OM/OC ratios for the relatively fresh biomass burning OA (BBOA) were 0.69 and 2.06, respectively, while the aged biomass burning OA (agBBOA) showed much higher elemental ratios~~

~~with O/C of 1.02 and OM/OC of 2.49. Correspondingly, the fragment also showed high contribution for agBBOA than that for BBOA (67.8% vs. 56.6%; Fig. S7). Although the *m/z* 44 (composed by) signals were still the highest peaks in both the two factors, the *m/z* 60 (composed by) signals which were generally regarded as well-known tracers for biomass burning emissions (Alfarra et al., 2007), were higher in BBOA than agBBOA HRMS (0.51% vs. 0.46%). In addition, both the fractions of in their HRMS were higher than the typical value of < 0.3% in the absence of biomass burning impacts (Cubison et al., 2011).~~ As shown in the Fig. 5, the time series of agBBOA correlated tightly with $C_2H_4O_2^+$ (R^2 = 0.79) and sulfate (R^2 = 0.47), while BBOA correlated slightly weak ~~corrected well~~ with $C_2H_4O_2^+$ (R^2 = 0.47) and potassium (R^2 = 0.30), respectively. The time series of agBBOA also correlated~~corrected~~ well with $C_xH_yO_1^+$ and $C_xH_yO_2^+$ ions, while BBOA correlated~~corrected~~ well with $C_xH_y^+$ and $C_xH_yO_1^+$ (Fig. ~~S8~~S10). In addition, both the mass spectra of the two biomass burning related OA factors resembled well with that of BBOA at QOMS (R^2 of 0.886 and 0.954, respectively; Fig. ~~S9~~S11; Zhang et al., 2018), whereas correlated ~~slightly weaker~~moderately (R^2 = 0.39–0.59) with other standard BBOA mass ~~spectrums~~ spectra at other sites around the world (Aiken et al., 2009; Mohr et al., 2012). The agBBOA mass spectrum in this study correlated tightly (R^2 = 0.914) with the less oxidized oxygenated OA (LOOOA) identified at Nam Co station (Fig. ~~S9~~S11; Xu et al., 2018). All these comparisons and correlation analysis further verified the reasonable source apportionment of OA in this study, namely there were two biomass burning related OAs at WLG, as a result of the different oxidation degrees of biomass burning emissions transported from surrounding areas to WLG site ~~which had different oxidation degrees likely due to their different sources and/or transport distances~~ (see Sect. 3.4 for details). Similar OA source apportionment of two BBOA components with different oxidation degrees have also been resolved in previous studies, e.g., an additional oxygenated biomass-burning-influenced organic aerosol (OOA_2-BBOA or OOA-BB) in the Paris metropolitan area (Crippa et al., 2013), urban Nanjing (Zhang et al., 2015) and Mt. Yulong (Zheng et al., 2017), respectively, besides the relatively fresh BBOA component. The O/C and OM/OC ratios for the relatively fresh biomass burning OA (BBOA) were 0.69 and 2.06, respectively, while much higher values of 1.02 and 2.49 for the aged biomass burning OA (agBBOA). Correspondingly, the $C_xH_yO_z^+$ fragment also showed higher contribution for agBBOA than that for BBOA (67.8% vs. 56.6%; Fig. S9). Moreover, the O/C ratio of BBOA in this study was also obviously higher than those in other urban or rural sites in China where had direct or local biomass burning sources, e.g., 0.24 in Lanzhou (Xu et al., 2016), 0.36 in Beijing (Sun et al., 2016) and 0.26 in Kaiping (Huang et al., 2011). The diurnal patterns of the two biomass burning related OAs presented nearly opposite trends in this study (Fig. 6c and d), with high values during the nighttime and decreased trend in the afternoon for BBOA whereas increased obviously during the daytime for agBBOA, mainly associated with the possible aging evolution from BBOA to agBBOA via photochemical oxidation during the daytime.

Another OA component, characterized by the highest peak at *m/z* 44 (contributed ~ 28% of total signal ~~and composed by C~~), the highest average O/C (1.42) and OM/OC (3.00), and the highest contribution of $C_xH_yO_z^+$ fragment (44.5% of $C_xH_yO_1^+$ and 30.6% of $C_xH_yO_2^+$; Fig. ~~S7~~S9) among the four factors, was identified as an oxygenated OA (OOA) in this study. The OOA HRMS in this study was quite similar with those more-oxidized oxygenated OA (MO-OOA) or low-volatility

oxygenated OA (LV-OOA) factors identified frequently in previous AMS studies, especially resembled tightly to those MO-OOA identified in other QTP locations (Fig. ~~S9~~S11), e.g. Nam Co (R^2 = 0.995; Xu et al., 2018) and QOMS (R^2 = 0.997; Zhang et al., 2018), suggesting that this factor mainly represented a typical regional oxygenated OA. The time series of OOA in this study correlated closely with the main secondary inorganic species, sulfate (R^2 = 0.51), indicating their commonly regional and aged properties. In addition, the time series of OOA also ~~corrected~~ correlated well with $C_xH_yO_2^+$ ions, especially with CO_2^+ (R^2 = 0.62) as shown in Fig. ~~S8~~S10. Although OOA showed relatively stable contributions throughout ~~during~~ the whole day, the ~~diurnal variation of~~ OOA mass concentrations also presented distinct diurnal variation at WLG site, namely relatively low values in the late morning, continuously increasing trend during the afternoon and moderate values ~~during~~ at the nighttime (Fig. 6c and d), ~~suggesting that OOA diurnal pattern was mainly driven by the combine effects of PBL variation and photochemical activities~~which tightly associated with the photochemical activities in the daytime, aqueous-processing of OA at nighttime as well as the diurnal variation of PBL height.

Overall, the average mass concentration of organics was 3.14 μg m^{-3} for the entire study and composed by 34.4% of OOA, 40.4% of agBBOA, 18.4% of BBOA and 6.8% of HOA on average (Fig. 6a). The biomass burning related OA components together contributed more than half of the total organics. In addition, obviously enhanced contributions were found for the two biomass burning related OA components, particular for agBBOA, with the increasing organics mass, whereas OOA decreased correspondingly (Fig. 6b). For example, BBOA and agBBOA contributed only ~ 10% to total organics when OA was less than 1.0 μg m^{-3}, whereas the contribution reached up to 70% with the mass concentration of OA increased to 7 μg m^{-3}. Moreover, the important contribution of agBBOA could also be clearly seen in the temporal variations in Fig. 2f, where agBBOA dominated organics during the relatively polluted periods. All of these suggested that biomass burning emissions from regional transport was the important source for OA at WLG. The triangle plot (*f*44 vs. *f*43 or fCO_2^+ vs. $fC_3H_3O^+$), which has been widely used in AMS studies, was an useful method to characterize the possible evolution mechanism of organic components upon aging in the ambient atmosphere (Ng et al., 2010). As shown in Fig. 4c and d, the majority of data are distributed within the two dash lines that defined as the general triangular space where ambient organic components fall by Ng et al. (2010). HOA presented relatively primary nature among four organic components and located in the bottom of triangle plots, while two biomass burning related components in the middle part and OOA in the upper-left corner of the triangle plots, suggesting an obvious oxidation evolution from relatively primary components to secondary components.

3.4 Source analysis

In order to study the dominant sources and explore the influence of regional transport to PM_1 mass loading and chemical composition at WLG during summer season, the 72 h backward air mass trajectories and average clusters at 500 m above ground level were calculated at 1 h intervals using the Hybrid Single Particle Lagrangian Integrated Trajectory (HYSPLIT) model (Draxler and Rolph, 2003) and meteorological data from the NOAA Global Data Assimilation System (GDAS). Finally, six air mass clusters were adopted in this study as presented in Fig. 7a.

Air masses from northeast (C1) with the shortest transport distance and lowest height among all the clusters, dominated the air mass contribution (57%) and had the highest average PM_1 mass concentration (10.8 μg m^{-3}) during the sampling period, whereas the rest five clusters (C2−C6) were generally from the west or northwest and showed apparently longer transport distances, higher heights and relatively lower mass concentrations (5.8−7.8 μg m^{-3}) than C1. As shown in Fig. 1b, three towns (Haiyan, Huangyuan and Huangzhong) as well as the capital city (Xining) of Qinghai Province were located to the northeast of WLG within 100 km, leading to relatively dense population and intense industrial activities in these areas compared with those areas to the west of WLG. Therefore, the prevailing air masses with low transport height for C1 could bring large amount of surface anthropogenic and industrial pollutants to WLG. This conclusion could further be supported by the significantly different contributions of chemical species during each cluster (Fig. 7a). Specifically, C1 showed higher contribution of sulfate compared to other clusters (39.5 vs. 32.0−35.5%), which was mainly related with the intense industrial emissions. In addition, OA components for C1 showed higher contributions from BBOA (19.5%) and agBBOA (43.3%) compared with those for C4 and C5 (12.3 and 11.2% for BBOA and 35.4 and 36.7% for agBBOA, respectively), whereas much lower contribution of oxidized OOA was found for C1 than those for C4 and C5 (31.0 vs. 43.9 and 44.0%), suggesting the relatively fresh of OA for C1. This phenomenon was more clear for the two distinct periods, P1 and P2, as shown in Fig. 7b and 8. Air masses for P2 was mainly from the northeast (C1; 79.0%) and resulted higher contributions from sulfate (39.9% to total PM_1) and the two biomass burning related OA components (BBOA and agBBOA, 63.2% to total organics), however, three clusters (C4−C6) from the west with long transport distances dominated P1 and led to significant enhancement of OOA contribution.

Besides the back trajectory analysis, bivariate polar plot analysis was another useful method to give insight into the potential source regions of ambient aerosols, which presents the relationships of mass concentrations of PM_1 chemical species with wind conditions (WS and WD) (Fig. ~~S10~~S12). All species showed elevated mass concentrations from east, however, with different hotspots for various species, suggesting their probably distinct sources and impacts from regional transport. The three main inorganic species (sulfate, nitrate and ammonium) and aged OOA generally had hotspots from the northeast in accordance with the predominant air masses from northeast during the daytime where showed more intensive anthropogenic and industrial emissions. Whereas chloride, BC and BBOA had obvious hotspots from southeast with wind speed around 10 m s^{-1}, which were mainly associated with the possible burning emissions of residents located to the southeast of WLG during the nighttime.

4 Conclusions

In this study, the highly time-resolved physicochemical properties of submicron aerosols were investigated during summer 2017 at a high-altitude background station in the northeastern QTP, using a suit of real-time instruments including HR-ToF-AMS, PAX, etc. The major findings include the following:

1. The ~~5 min~~ mass concentration of total PM_1 (NR-PM_1 + BC) varied dynamically between 0.3 and 28.1 μg m^{-3} during this study, with an average PM_1 mass loading of 9.1 (± 5.3) μg m^{-3},

which was higher than those measured with Aerodyne AMS at other high-elevation sites in the southern or central QTP. Different with the significant impacts of biomass burning emissions in the southern QTP, sulfate showed dominant contribution (38.1%) at WLG. In addition, mass contribution of sulfate increased obviously with the increase of PM_1 mass loading, indicating the apparently regional transport of sulfate from industrial ~~inland~~ areas in the northwestern China. Correspondingly, PM_1 appeared to be slightly acidic throughout this study related with the enhanced sulfate contribution. All chemical species of NR-PM_1 peaked at the accumulation mode, suggesting the well mixed and highly aged aerosol particles at WLG during the sampling period.

2. OA on average was dominated by 65.7% of $C_xH_yO_z^+$ ion fragment, with the average O/C ratio of 0.99 and OM/OC ratio of 2.44, indicating its highly aged property at this remote site. PMF analysis performed on the OA HRMS resolved four distinct OA components, including HOA, BBOA, agBBOA and OOA. On average, the two relatively oxidized OAs (OOA and agBBOA) contributed 34.4% and 40.4%, respectively, while the rest were 18.4% for BBOA and 6.8% for HOA. In addition, obvious enhanced contributions were found for the two biomass burning related OA components with the increasing OA mass, demonstrating that biomass burning emissions from regional transport was the dominant OA source at WLG.

3. Air masses from northeast (C1) with the shortest transport distance among the six clusters presented dominant contribution (57%) and the highest PM_1 mass concentration (10.8 μg m^{-3}), mainly due to the enhanced contributions of sulfate and biomass burning related OA components from the industrial ~~inland~~ areas in the northwestern China. The rest clusters (C2−C6) from the west or northwest with apparently larger transport distances, however, showed relatively lower mass concentrations and higher OOA contributions than C1. These source analysis together suggested the distinct aerosol sources and significant impacts of regional transport to aerosol mass loadings and chemical compositions at WLG during summer season.

Data availability. The processed AMS data and meteorological data in this study are available upon request from the corresponding author.

Author contribution. XHZ analyzed the data and wrote the manuscript. JZX organized the campaign, analyzed data, and wrote the manuscript. SCK and QZ wrote the manuscript.

Acknowledgements. The authors thank the Waliguan Baseline Observatory for the logistical support with the field campaign and thank the colleagues for continuing support and discussion. This research was supported by grants from the National Natural Science Foundation of China (41771079), the Strategic Priority Research Program of Chinese Academy of Sciences, Pan-Third Pole Environment Study for a Green Silk Road (Pan-TPE) (XDA20040501), and the Chinese Academy of Sciences Hundred Talents Program.

References

Aiken, A. C., DeCarlo, P. F., Kroll, J. H., Worsnop, D. R., Huffman, J. A., Docherty, K. S., Ulbrich, I. M., Mohr, C., Kimmel, J.

R., Sueper, D., Sun, Y., Zhang, Q., Trimborn, A., Northway, M., Ziemann, P. J., Canagaratna, M. R., Onasch, T. B., Alfarra, M. R., Prevot, A. S. H., Dommen, J., Duplissy, J., Metzger, A., Baltensperger, U., and Jimenez, J. L.: O/C and OM/OC ratios of primary, secondary, and ambient organic aerosols with high-resolution time-of-flight aerosol mass spectrometry, Environ. Sci. Technol., 42, 4478-4485, doi:10.1021/es703009q, 2008.

Aiken, A. C., Salcedo, D., Cubison, M. J., Huffman, J. A., DeCarlo, P. F., Ulbrich, I. M., Docherty, K. S., Sueper, D., Kimmel, J. R., Worsnop, D. R., Trimborn, A., Northway, M., Stone, E. A., Schauer, J. J., Volkamer, R. M., Fortner, E., de Foy, B., Wang, J., Laskin, A., Shutthanandan, V., Zheng, J., Zhang, R., Gaffney, J., Marley, N. A., Paredes-Miranda, G., Arnott, W. P., Molina, L. T., Sosa, G., and Jimenez, J. L.: Mexico City aerosol analysis during MILAGRO using high resolution aerosol mass spectrometry at the urban supersite (T0)–Part 1: Fine particle composition and organic source apportionment, Atmos. Chem. Phys., 9, 6633-6653, doi:10.5194/acp-9-6633-2009, 2009.

Alfarra, M. R., Prevot, A. S. H., Szidat, S., Sandradewi, J., Weimer, S., Lanz, V. A., Schreiber, D., Mohr, M., and Baltensperger, U.: Identification of the Mass Spectral Signature of Organic Aerosols from Wood Burning Emissions, Environ. Sci. Technol., 41, 5770-5777, doi:10.1021/es062289b, 2007.

Canagaratna, M. R., Jayne, J. T., Jimenez, J. L., Allan, J. D., Alfarra, M. R., Zhang, Q., Onasch, T. B., Drewnick, F., Coe, H., Middlebrook, A., Delia, A., Williams, L. R., Trimborn, A. M., Northway, M. J., DeCarlo, P. F., Kolb, C. E., Davidovits, P., and Worsnop, D. R.: Chemical and microphysical characterization of ambient aerosols with the aerodyne aerosol mass spectrometer, Mass Spectrom. Rev., 26, 185-222, doi:10.1002/mas.20115, 2007.

Canagaratna, M. R., Jimenez, J. L., Kroll, J. H., Chen, Q., Kessler, S. H., Massoli, P., Hildebrandt Ruiz, L., Fortner, E., Williams, L. R., Wilson, K. R., Surratt, J. D., Donahue, N. M., Jayne, J. T., and Worsnop, D. R.: Elemental ratio measurements of organic compounds using aerosol mass spectrometry: characterization, improved calibration, and implications, Atmos. Chem. Phys., 15, 253-272, doi:10.5194/acp-15-253-2015, 2015.

Crippa, M., DeCarlo, P. F., Slowik, J. G., Mohr, C., Heringa, M. F., Chirico, R., Poulain, L., Freutel, F., Sciare, J., Cozic, J., Di Marco, C. F., Elsasser, M., Nicolas, J. B., Marchand, N., Abidi, E., Wiedensohler, A., Drewnick, F., Schneider, J., Borrmann, S., Nemitz, E., Zimmermann, R., Jaffrezo, J. L., Prévôt, A. S. H., and Baltensperger, U.: Wintertime aerosol chemical composition and source apportionment of the organic fraction in the metropolitan area of Paris, Atmos. Chem. Phys., 13, 961-981, doi:10.5194/acp-13-961-2013, 2013.

Cubison, M. J., Ortega, A. M., Hayes, P. L., Farmer, D. K., Day, D., Lechner, M. J., Brune, W. H., Apel, E., Diskin, G. S., Fisher, J. A., Fuelberg, H. E., Hecobian, A., Knapp, D. J., Mikoviny, T., Riemer, D., Sachse, G. W., Sessions, W., Weber, R. J., Weinheimer, A. J., Wisthaler, A., and Jimenez, J. L.: Effects of aging on organic aerosol from open biomass burning smoke in aircraft and laboratory studies, Atmos. Chem. Phys., 11, 12049-12064, doi:10.5194/acp-11-12049-2011, 2011.

DeCarlo, P. F., Kimmel, J. R., Trimborn, A., Northway, M. J., Jayne, J. T., Aiken, A. C., Gonin, M., Fuhrer, K., Horvath, T., Docherty, K. S., Worsnop, D. R., and Jimenez, J. L.: Field-Deployable, High-Resolution, Time-of-Flight Aerosol Mass Spectrometer, Anal. Chem., 78, 8281-8289, doi:10.1021/ac061249n, 2006.

Draxler, R. R., and Rolph, G. D.: HYSPLIT (HYbrid Single-Particle Lagrangian Integrated Trajectory) model access via NOAA ARL READY website (http://www.arl.noaa.gov/ready/hysplit4.html). NOAA Air Resources Laboratory, Silver Spring, MD, USA, 2003.

Du, W., Sun, Y. L., Xu, Y. S., Jiang, Q., Wang, Q. Q., Yang, W., Wang, F., Bai, Z. P., Zhao, X. D., and Yang, Y. C.: Chemical characterization of submicron aerosol and particle growth events at a national background site (3295 m a.s.l.) on the Tibetan Plateau, Atmos. Chem. Phys., 15, 10811-10824, doi:10.5194/acp-15-10811-2015, 2015.

Elser, M., Huang, R.-J., Wolf, R., Slowik, J. G., Wang, Q., Canonaco, F., Li, G., Bozzetti, C., Daellenbach, K. R., Huang, Y., Zhang, R., Li, Z., Cao, J., Baltensperger, U., El-Haddad, I., and Prévôt, A. S. H.: New insights into PM_{2.5} chemical composition and sources in two major cities in China during extreme haze events using aerosol mass spectrometry, Atmos. Chem. Phys., 16, 3207-3225, doi:10.5194/acp-16-3207-2016, 2016.

Engling, G., Zhang, Y. N., Chan, C. Y., Sang, X. F., Lin, M., Ho, K. F., Li, Y. S., Lin, C. Y., and Lee, J. J.: Characterization and sources of aerosol particles over the southeastern Tibetan Plateau during the Southeast Asia biomass-burning season, Tellus B, 63, 117-128, doi:10.1111/j.1600-0889.2010.00512.x, 2011.

He, L. Y., Lin, Y., Huang, X. F., Guo, S., Xue, L., Su, Q., Hu, M., Luan, S. J., and Zhang, Y. H.: Characterization of high-resolution aerosol mass spectra of primary organic aerosol emissions from Chinese cooking and biomass burning, Atmos. Chem. Phys., 10, 11535-11543, doi:10.5194/acp-10-11535-2010, 2010.

Heald, C. L., Kroll, J. H., Jimenez, J. L., Docherty, K. S., DeCarlo, P. F., Aiken, A. C., Chen, Q., Martin, S. T., Farmer, D. K., and Artaxo, P.: A simplified description of the evolution of organic aerosol composition in the atmosphere, Geophys. Res. Lett., 37, L08803, doi:10.1029/2010gl042737, 2010.

Hu, W., Hu, M., Hu, W.-W., Zheng, J., Chen, C., Wu, Y., and Guo, S.: Seasonal variations in high time-resolved chemical compositions, sources, and evolution of atmospheric submicron aerosols in the megacity Beijing, Atmos. Chem. Phys., 17, 9979-10000, doi:10.5194/acp-17-9979-2017, 2017.

Hu, W. W., Hu, M., Hu, W., Jimenez, J. L., Yuan, B., Chen, W., Wang, M., Wu, Y., Chen, C., Wang, Z., Peng, J., Zeng, L., and Shao, M.: Chemical composition, sources, and aging process of submicron aerosols in Beijing: Contrast between summer and winter, J. Geophys. Res. Atmos., 121, 1955-1977, doi:10.1002/2015jd024020, 2016.

Huang, X. F., He, L. Y., Hu, M., Canagaratna, M. R., Kroll, J. H., Ng, N. L., Zhang, Y. H., Lin, Y., Xue, L., Sun, T. L., Liu, X. G., Shao, M., Jayne, J. T., and Worsnop, D. R.: Characterization of submicron aerosols at a rural site in Pearl River Delta of China using an Aerodyne High-Resolution Aerosol Mass Spectrometer, Atmos. Chem. Phys., 11, 1865-1877, doi:10.5194/acp-11-1865-2011, 2011.

Jayne, J. T., Leard, D. C., Zhang, X. F., Davidovits, P., Smith, K. A., Kolb, C. E., and Worsnop, D. R.: Development of an aerosol mass spectrometer for size and composition analysis of submicron particles, Aerosol Sci. Technol., 33, 49-70, doi:10.1080/027868200410840, 2000.

Jimenez, J. L., Jayne, J. T., Shi, Q., Kolb, C. E., Worsnop, D. R., Yourshaw, I., Seinfeld, J. H., Flagan, R. C., Zhang, X., Smith, K. A., Morris, J. W., and Davidovits, P.: Ambient aerosol sampling using the Aerodyne Aerosol Mass Spectrometer, J. Geophys. Res., 108, 8425, doi:10.1029/2001jd001213, 2003.

Kang, S., Xu, Y., You, Q., Flügel, W.-A., Pepin, N., and Yao, T.: Review of climate and cryospheric change in the Tibetan Plateau, Environ. Res. Lett., 5, 015101, doi:10.1088/1748-9326/5/1/015101, 2010.

Li, C., Bosch, C., Kang, S., Andersson, A., Chen, P., Zhang, Q., Cong, Z., Chen, B., Qin, D., and Gustafsson, O.: Sources of black carbon to the Himalayan-Tibetan Plateau glaciers, Nat. Commun., 7, 12574, doi:10.1038/ncomms12574, 2016.

Li, J., Wang, G., Wang, X., Cao, J., Sun, T., Cheng, C., Meng, J., Hu, T., and Liu, S.: Abundance, composition and source of atmospheric PM2.5 at a remote site in the Tibetan Plateau, China, Tellus B: Chemical and Physical Meteorology, 65, 20281, doi:10.3402/tellusb.v65i0.20281, 2013.

Li, Y. J., Sun, Y., Zhang, Q., Li, X., Li, M., Zhou, Z., and Chan, C. K.: Real-time chemical characterization of atmospheric particulate matter in China: A review, Atmos. Environ., 158, 270-304, doi:10.1016/j.atmosenv.2017.02.027, 2017.
Lu, Z., Zhang, Q., and Streets, D. G.: Sulfur dioxide and primary carbonaceous aerosol emissions in China and India, 1996–2010, Atmos. Chem. Phys., 11, 9839-9864, doi:10.5194/acp-11-9839-2011, 2011.
Lüthi, Z. L., Škerlak, B., Kim, S. W., Lauer, A., Mues, A., Rupakheti, M., and Kang, S.: Atmospheric brown clouds reach the Tibetan Plateau by crossing the Himalayas, Atmos. Chem. Phys., 15, 6007-6021, doi:10.5194/acp-15-6007-2015, 2015.
Middlebrook, A. M., Bahreini, R., Jimenez, J. L., and Canagaratna, M. R.: Evaluation of Composition-Dependent Collection Efficiencies for the Aerodyne Aerosol Mass Spectrometer using Field Data, Aerosol Sci. Technol., 46, 258-271, doi:10.1080/02786826.2011.620041, 2012.
Mohr, C., DeCarlo, P. F., Heringa, M. F., Chirico, R., Slowik, J. G., Richter, R., Reche, C., Alastuey, A., Querol, X., Seco, R., Peñuelas, J., Jiménez, J. L., Crippa, M., Zimmermann, R., Baltensperger, U., and Prévôt, A. S. H.: Identification and quantification of organic aerosol from cooking and other sources in Barcelona using aerosol mass spectrometer data, Atmos. Chem. Phys., 12, 1649-1665, doi:10.5194/acp-12-1649-2012, 2012.
Ng, N. L., Canagaratna, M. R., Zhang, Q., Jimenez, J. L., Tian, J., Ulbrich, I. M., Kroll, J. H., Docherty, K. S., Chhabra, P. S., Bahreini, R., Murphy, S. M., Seinfeld, J. H., Hildebrandt, L., Donahue, N. M., DeCarlo, P. F., Lanz, V. A., Prévôt, A. S. H., Dinar, E., Rudich, Y., and Worsnop, D. R.: Organic aerosol components observed in Northern Hemispheric datasets from Aerosol Mass Spectrometry, Atmos. Chem. Phys., 10, 4625-4641, doi:10.5194/acp-10-4625-2010, 2010.
Ng, N. L., Canagaratna, M. R., Jimenez, J. L., Zhang, Q., Ulbrich, I. M., and Worsnop, D. R.: Real-time methods for estimating organic component mass concentrations from aerosol mass spectrometer data, Environ. Sci. Technol., 45, 910-916, doi:10.1021/es102951k, 2011.
Paatero, P., and Tapper, U.: Positive matrix factorization: A non-negative factor model with optimal utilization of error estimates of data values, Environmetrics, 5, 111-126, doi:10.1002/env.3170050203, 1994.
Qian, Y., Flanner, M. G., Leung, L. R., and Wang, W.: Sensitivity studies on the impacts of Tibetan Plateau snowpack pollution on the Asian hydrological cycle and monsoon climate, Atmos. Chem. Phys., 11, 1929-1948, doi:10.5194/acp-11-1929-2011, 2011.
Sun, Y. L., Zhang, Q., Schwab, J. J., Demerjian, K. L., Chen, W. N., Bae, M. S., Hung, H. M., Hogrefe, O., Frank, B., Rattigan, O. V., and Lin, Y. C.: Characterization of the sources and processes of organic and inorganic aerosols in New York city with a high-resolution time-of-flight aerosol mass apectrometer, Atmos. Chem. Phys., 11, 1581-1602, doi:10.5194/acp-11-1581-2011, 2011.
Sun, Y. L., Du, W., Fu, P., Wang, Q., Li, J., Ge, X., Zhang, Q., Zhu, C., Ren, L., Xu, W., Zhao, J., Han, T., Worsnop, D. R., and Wang, Z.: Primary and secondary aerosols in Beijing in winter: sources, variations and processes, Atmos. Chem. Phys., 16, 8309-8329, doi:10.5194/acp-16-8309-2016, 2016.
Ulbrich, I. M., Canagaratna, M. R., Zhang, Q., Worsnop, D. R., and Jimenez, J. L.: Interpretation of organic components from Positive Matrix Factorization of aerosol mass spectrometric data, Atmos. Chem. Phys., 9, 2891-2918, doi:10.5194/acp-9-2891-2009, 2009.
van der A, R. J., Mijling, B., Ding, J., Koukouli, M. E., Liu, F., Li, Q., Mao, H., and Theys, N.: Cleaning up the air: effectiveness of air quality policy for SO₂ and NO_{<i>x</i>} emissions in China, Atmos. Chem. Phys., 17, 1775-1789, doi:10.5194/acp-17-1775-2017, 2017.
Wang, J., Zhang, Q., Chen, M., Collier, S., Zhou, S., Ge, X., Xu, J., Shi, J., Xie, C., Hu, J., Ge, S., Sun, Y., and Coe, H.: First Chemical Characterization of Refractory Black Carbon Aerosols and Associated Coatings over the Tibetan Plateau (4730 m a.s.l), Environ. Sci. Technol., 51, 14072-14082, doi:10.1021/acs.est.7b03973, 2017.
Xia, X., Zong, X., Cong, Z., Chen, H., Kang, S., and Wang, P.: Baseline continental aerosol over the central Tibetan plateau and a case study of aerosol transport from South Asia, Atmos. Environ., 45, 7370-7378, doi:10.1016/j.atmosenv.2011.07.067, 2011.
Xu, B., Cao, J., Hansen, J., Yao, T., Joswia, D. R., Wang, N., Wu, G., Wang, M., Zhao, H., Yang, W., Liu, X., and He, J.: Black soot and the survival of Tibetan glaciers, Proc. Natl. Acad. Sci. USA, 106, 22114-22118, doi:10.1073/pnas.0910444106, 2009.
Xu, J., Wang, Z., Yu, G., Sun, W., Qin, X., Ren, J., and Qin, D.: Seasonal and diurnal variations in aerosol concentrations at a high-altitude site on the northern boundary of Qinghai-Xizang Plateau, Atmos. Res., 120-121, 240-248, doi:10.1016/j.atmosres.2012.08.022, 2013.
Xu, J., Wang, Z., Yu, G., Qin, X., Ren, J., and Qin, D.: Characteristics of water soluble ionic species in fine particles from a high altitude site on the northern boundary of Tibetan Plateau: Mixture of mineral dust and anthropogenic aerosol, Atmos. Res., 143, 43-56, doi:http://dx.doi.org/10.1016/j.atmosres.2014.01.018, 2014a.
Xu, J., Zhang, Q., Chen, M., Ge, X., Ren, J., and Qin, D.: Chemical composition, sources, and processes of urban aerosols during summertime in northwest China: insights from high-resolution aerosol mass spectrometry, Atmos. Chem. Phys., 14, 12593-12611, doi:10.5194/acp-14-12593-2014, 2014b.
Xu, J., Zhang, Q., Wang, Z. B., Yu, G. M., Ge, X. L., and Qin, X.: Chemical composition and size distribution of summertime $PM_{2.5}$ at a high altitude remote location in the northeast of the Qinghai–Xizang (Tibet) Plateau: insights into aerosol sources and processing in free troposphere, Atmos. Chem. Phys., 15, 5069-5081, doi:10.5194/acp-15-5069-2015, 2015.
Xu, J., Shi, J., Zhang, Q., Ge, X., Canonaco, F., Prévôt, A. S. H., Vonwiller, M., Szidat, S., Ge, J., Ma, J., An, Y., Kang, S., and Qin, D.: Wintertime organic and inorganic aerosols in Lanzhou, China: sources, processes, and comparison with the results during summer, Atmos. Chem. Phys., 16, 14937-14957, doi:10.5194/acp-16-14937-2016, 2016.
Xu, J., Zhang, Q., Shi, J., Ge, X., Xie, C., Wang, J., Kang, S., Zhang, R., and Wang, Y.: Chemical characteristics of submicron particles at the central Tibetan Plateau: insights from aerosol mass spectrometry, Atmos. Chem. Phys., 18, 427-443, doi:10.5194/acp-18-427-2018, 2018.
Xue, L. K., Wang, T., Guo, H., Blake, D. R., Tang, J., Zhang, X. C., Saunders, S. M., and Wang, W. X.: Sources and photochemistry of volatile organic compounds in the remote atmosphere of western China: results from the Mt. Waliguan Observatory, Atmos. Chem. Phys., 13, 8551-8567, doi:10.5194/acp-13-8551-2013, 2013.
Yang, K., Wu, H., Qin, J., Lin, C., Tang, W., and Chen, Y.: Recent climate changes over the Tibetan Plateau and their impacts on energy and water cycle: A review, Global and Planetary Change, 112, 79-91, doi:10.1016/j.gloplacha.2013.12.001, 2014.
Yao, T., Thompson, L., Mosbrugger, V., Zhang, F., Ma, Y., Luo, T., Xu, B., Yang, X., Joswiak, D. R., Wang, W., Joswiak, M. E., Devkota, L. P., Tayal, S., Jilani, R., and Fayziev, R.: Third Pole Environment (TPE), Environmental Development, 3, 52-64, doi:10.1016/j.envdev.2012.04.002, 2012.
Zhang, N., Cao, J., Liu, S., Zhao, Z., Xu, H., and Xiao, S.: Chemical composition and sources of PM2.5 and TSP collected at Qinghai Lake during summertime, Atmos. Res., 138, 213-222, doi:10.1016/j.atmosres.2013.11.016, 2014.
Zhang, Q., Worsnop, D., Canagaratna, M., and Jimenez, J.: Hydrocarbon-like and oxygenated organic aerosols in Pittsburgh: insights into sources and processes of organic aerosols, Atmos. Chem. Phys., 5, 3289-3311, doi:10.5194/acp-5-3289-2005,

2005.~~Zhang, Q., Canagaratna, M. R., Jayne, J. T., Worsnop, D. R., and Jimenez, J. L.: Time- and size-resolved chemical composition of submicron particles in Pittsburgh: Implications for aerosol sources and processes, J. Geophys. Res., 110, D07S09, doi:10.1029/2004jd004649, 2005.~~

Zhang, Q., Jimenez, J. L., Worsnop, D. R., and Canagaratna, M.: A case study of urban particle acidity and its influence on secondary organic aerosol, Environ. Sci. Technol., 41, 3213-3219, doi:10.1021/es061812j, 2007.

Zhang, Q., Jimenez, J. L., Canagaratna, M. R., Ulbrich, I. M., Ng, N. L., Worsnop, D. R., and Sun, Y.: Understanding atmospheric organic aerosols via factor analysis of aerosol mass spectrometry: a review, Anal. Bioanal. Chem., 401, 3045-3067, doi:10.1007/s00216-011-5355-y, 2011.

Zhang, R., Wang, Y., He, Q., Chen, L., Zhang, Y., Qu, H., Smeltzer, C., Li, J., Alvarado, L. M. A., Vrekoussis, M., Richter, A., Wittrock, F., and Burrows, J. P.: Enhanced trans-Himalaya pollution transport to the Tibetan Plateau by cut-off low systems, Atmos. Chem. Phys., 17, 3083-3095, doi:10.5194/acp-17-3083-2017, 2017.

Zhang, X., Xu, J., Kang, S., Liu, Y., and Zhang, Q.: Chemical characterization of long-range transport biomass burning emissions to the Himalayas: insights from high-resolution aerosol mass spectrometry, Atmos. Chem. Phys., 18, 4617-4638, doi:10.5194/acp-18-4617-2018, 2018.

Zhang, Y. J., Tang, L. L., Wang, Z., Yu, H. X., Sun, Y. L., Liu, D., Qin, W., Canonaco, F., Prévôt, A. S. H., Zhang, H. L., and Zhou, H. C.: Insights into characteristics, sources, and evolution of submicron aerosols during harvest seasons in the Yangtze River delta region, China, Atmos. Chem. Phys., 15, 1331-1349, doi:10.5194/acp-15-1331-2015, 2015.

Zheng, J., Hu, M., Du, Z., Shang, D., Gong, Z., Qin, Y., Fang, J., Gu, F., Li, M., Peng, J., Li, J., Zhang, Y., Huang, X., He, L., Wu, Y., and Guo, S.: Influence of biomass burning from South Asia at a high-altitude mountain receptor site in China, Atmos. Chem. Phys., 17, 6853-6864, doi:10.5194/acp-17-6853-2017, 2017.

Zhou, S., Collier, S., Jaffe, D. A., Briggs, N. L., Hee, J., Sedlacek Iii, A. J., Kleinman, L., Onasch, T. B., and Zhang, Q.: Regional influence of wildfires on aerosol chemistry in the western US and insights into atmospheric aging of biomass burning organic aerosol, Atmos. Chem. Phys., 17, 2477–2493, https://doi.org/10.5194/acp-17-2477-2017, 2017.

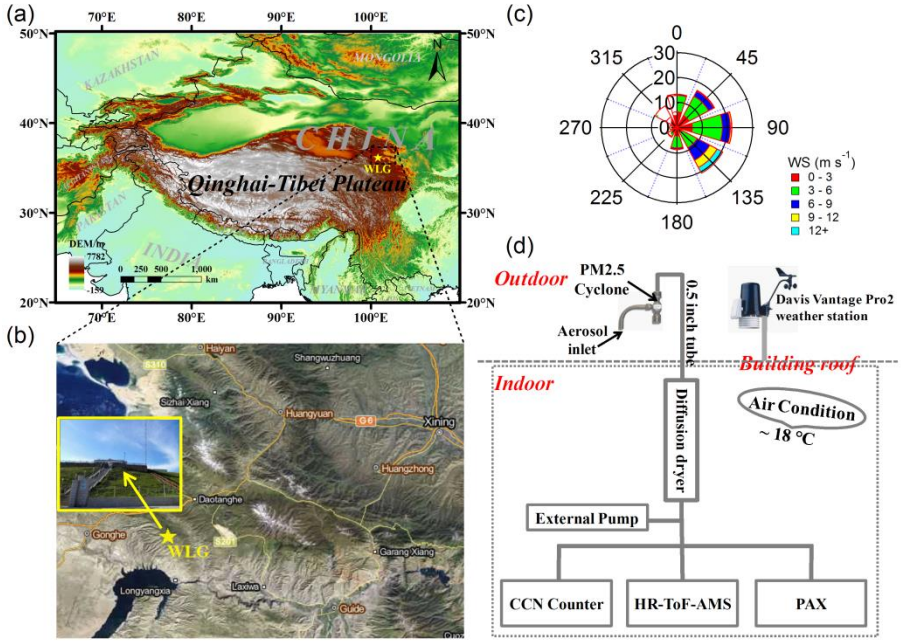

Figure 1. (a) Topography map of the Qinghai-Tibet Plateau (QTP), **(b)** location map of Mt. Waliguan Base (WLG; 36.283° N, 100.900° E, 3816 m), **(c)** the wind rose plot colored by wind speed during the field study period, and **(d)** the setup of instruments in this study.

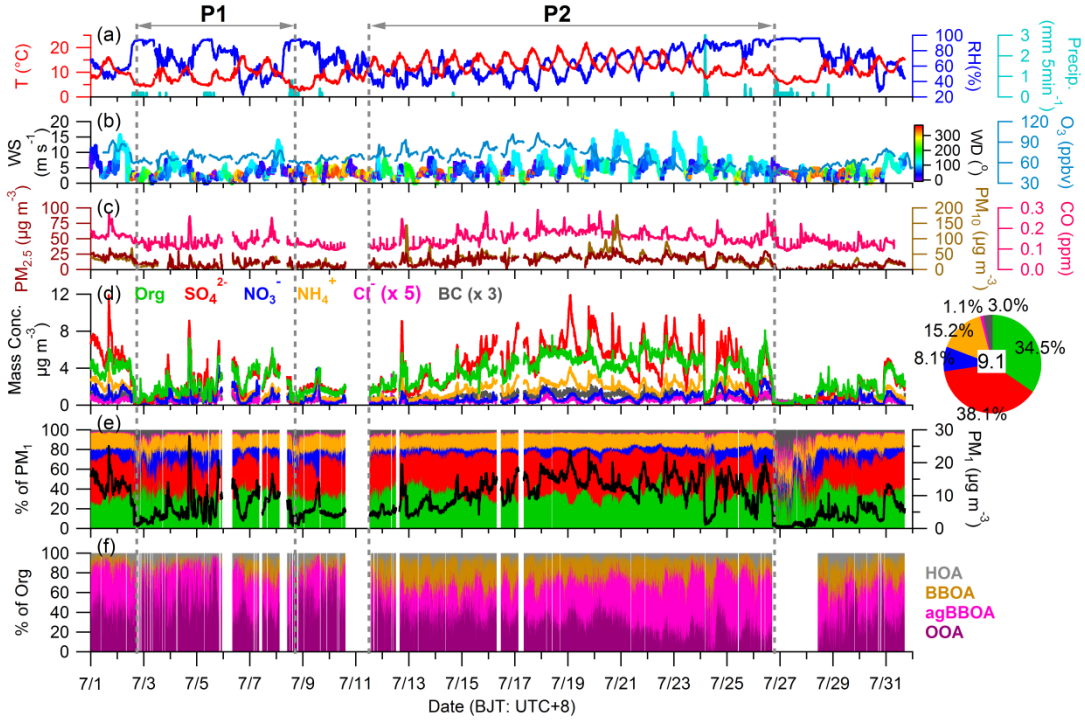

Figure 2. Time series of **(a)** ambient temperature (*T*), relative humidity (RH), and precipitation (Precip.), **(b)** wind speed (WS) colored by wind direction (WD) and O_3, **(c)** mass concentrations of $PM_{2.5}$, PM_{10}, and CO, **(d)** mass concentrations of PM_1 species, **(e)** mass contributions of PM_1 species as well as the total PM_1 mass concentrations, **(f)** mass contributions of four organic components. The pie chart shows the average chemical composition of PM_1 for the entire study period, with the average PM_1 mass concentration (unit of μg m^{-3}) marked in the central.

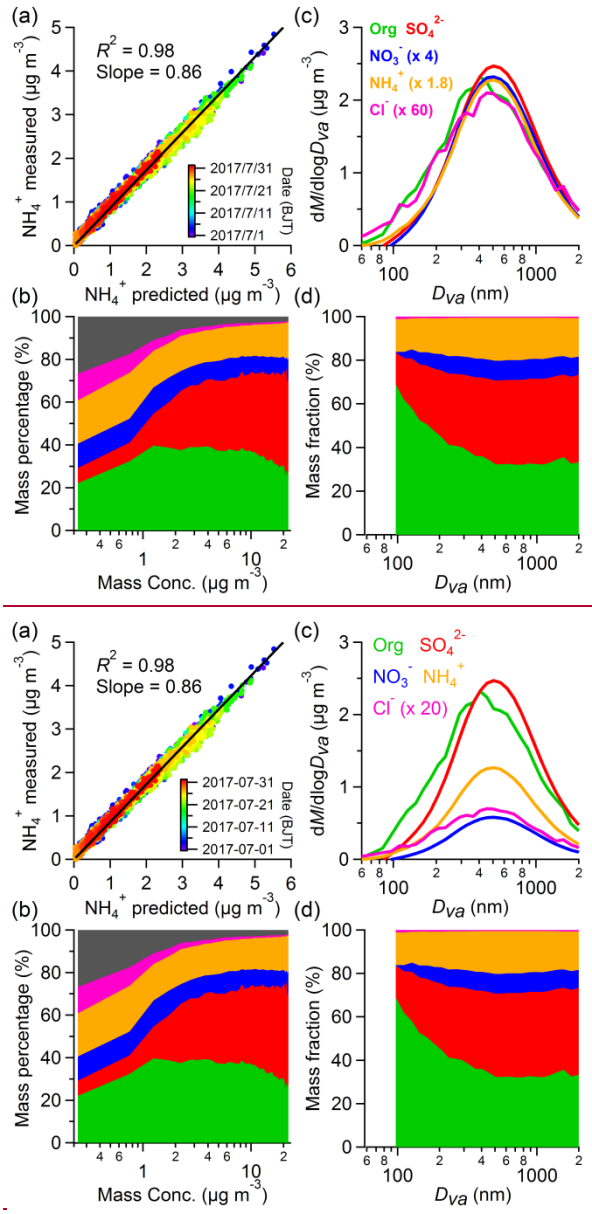

Figure 3. (a) Scatterplot and linear regression (black solid line) of measured NH_4^+ versus predicted NH_4^+ based on the mass concentrations of SO_4^{2-}, NO_3^-, and Cl^-, **(b)** the mass contributions of PM_1 chemical species as a function of total PM_1 mass concentration, and the average size distributions of **(c)** mass concentrations and **(d)** mass contributions of NR-PM_1 species in this study.

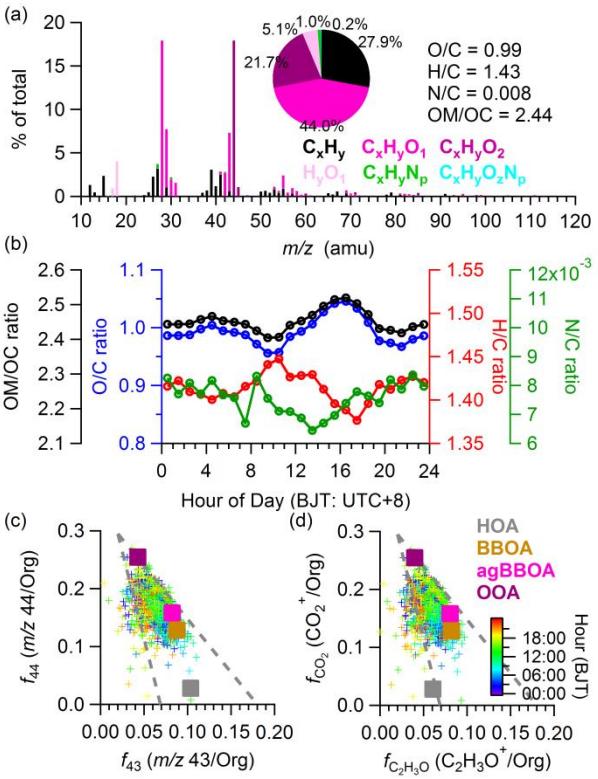

758

759 **Figure 4. (a)** The average high-resolution mass spectrum of organics colored with six ion categories (pie charts shows the
760 average contributions of the six ion categories), **(b)** diurnal variations of element ratios (O/C, H/C, N/C, and OM/OC), and
761 scatterplots of **(c)** *f*44 vs. *f*43 and **(d)** fCO_2^+ vs. $fC_2H_3O^+$ colored by time of the day, where the corresponding values of four
762 organic components are also shown.

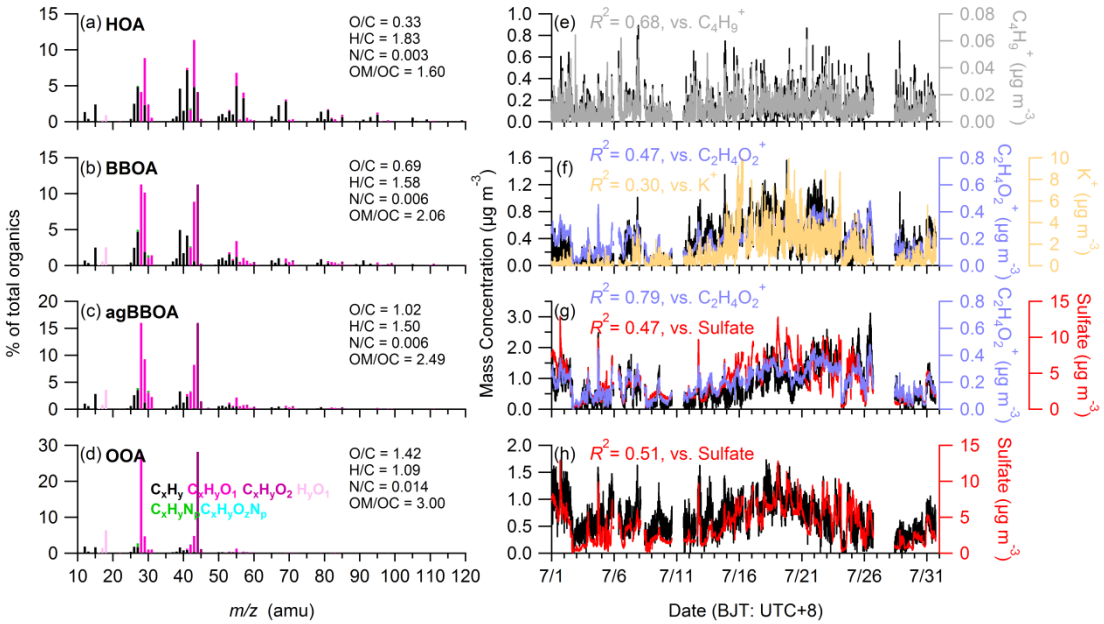

763

764 **Figure 5.** PMF results of **(left)** high-resolution mass spectra colored by six ion categories for the four OA factors at *m*/*z* < 120,
765 **(right)** temporal variations of the four OA factors and corresponding comparison with tracer species.

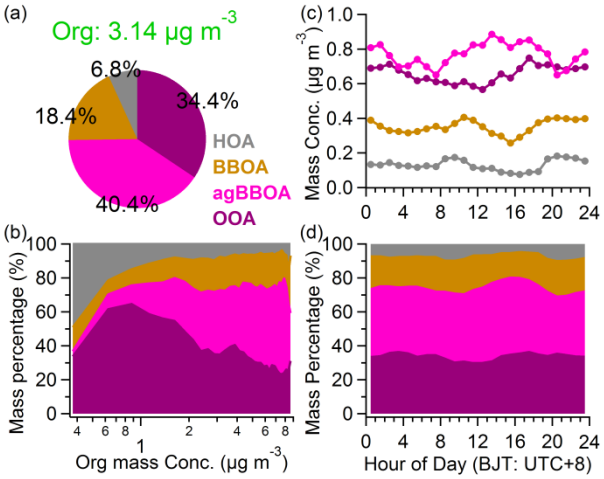

766

767 **Figure 6.** The average mass contributions of four organic components to total organics **(a)** during the entire study period and **(b)**
768 as a function of total organics mass concentrations, as well as the diurnal variations of **(c)** mass concentrations and **(d)** mass
769 contributions of four organic components in this study.

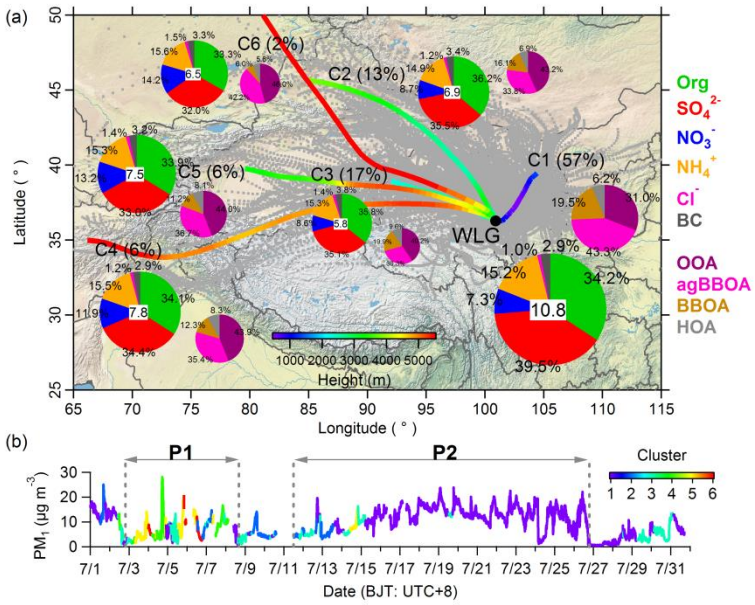

770

771 **Figure 7. (a)** The 72h backward air mass trajectories (grey dotted lines) and average trajectory clusters (solid lines colored
772 according to height) calculated at 1 h intervals for the entire study period. Pie charts show the average mass contributions of PM_1
773 species to total PM_1 (average PM_1 mass are marked in the central of pie charts) and OA components to total organics belong to
774 each cluster (areas of pie charts are scaled by the corresponding average mass), respectively. **(b)** Temporal variation of PM_1 mass
775 concentration colored by the corresponding cluster name in this study. The markers of P1 and P2 represent two different periods
776 that selected in this study.

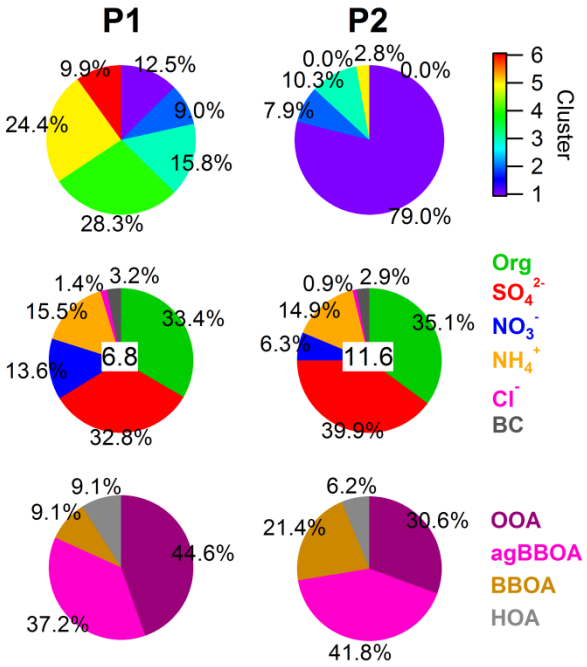

Figure 8. (a) The occurrence frequency of six air mass trajectory clusters, **(b)** average contributions of PM_1 chemical species to total PM_1, and **(c)** average contributions of four organic components to total organics during P1 and P2, respectively.

Supplement of

Chemical characterization and sources of submicron aerosols in the northeastern Qinghai-Tibet Plateau: insights from high-resolution mass spectrometry

Xinghua Zhang et al.

Correspondence to: Jianzhong Xu (jzxu@lzb.ac.cn)

Figures

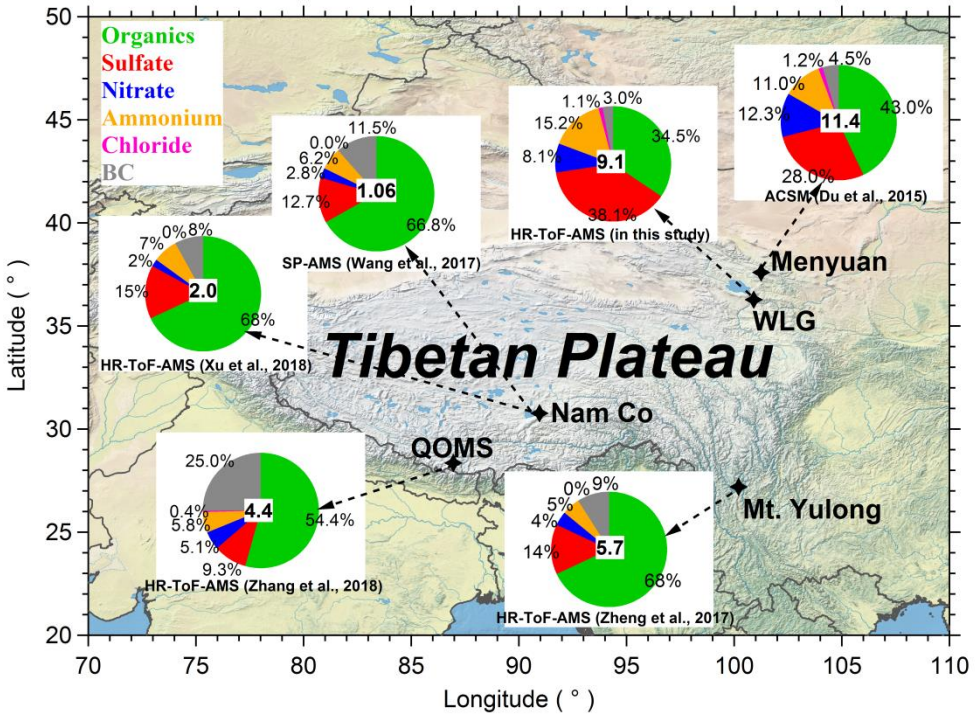

Figure S1. The field studies conducted at high elevation sites in the Qinghai-Tibet Plateau using AMS or ACSM measurements. The mass concentrations of PM_1 and the mass contributions of each chemical species (pie chart) are presented in each site.

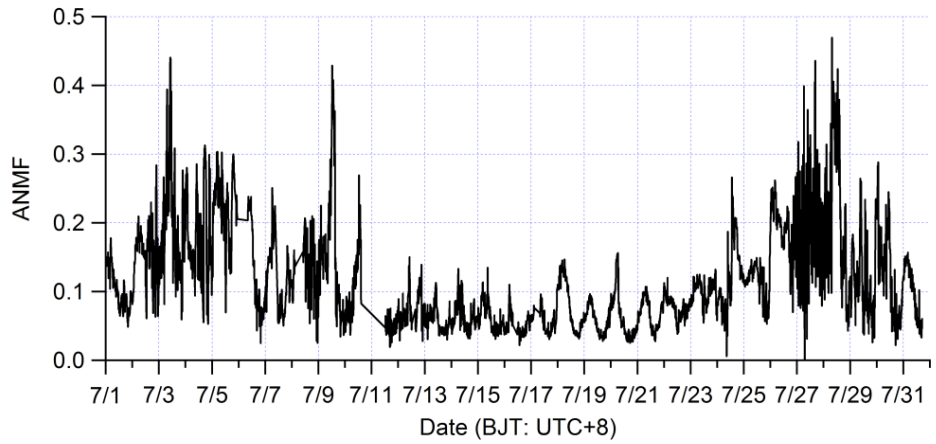

Figure ~~S1~~S2. The time series of ANMF (ANMF = (80/62×NO_3)/(NH_4 + SO_4 + NO_3 + Chl + Org)) in this study.

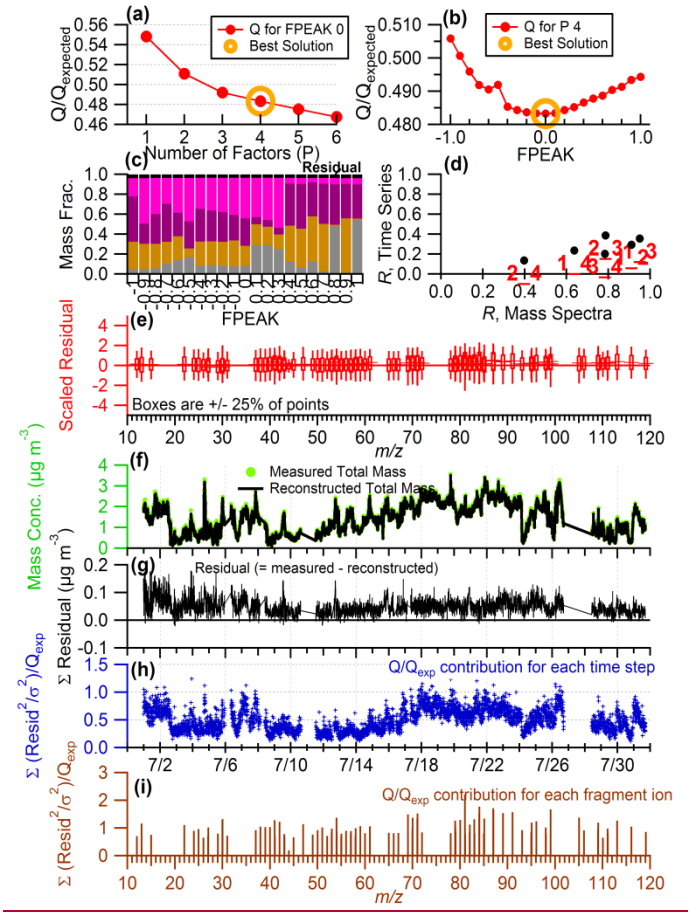

Figure S3. Summary of key diagnostic plots of the PMF results: **(a)** Q/Q_{exp} as a function of factor number (p) that selected for PMF analysis. For the best solution (four factors solution): **(b)** Q/Q_{exp} as a function of *f*Peak, **(c)** fractions of OA factors vs. *f*Peak, **(d)** correlations among PMF factors, **(e)** the box and whiskers plot showing the distributions of scaled residuals for each m/z, **(f)** time series of the measured organic mass and the reconstructed organic mass, **(g)** variations of the residual (= measured - reconstructed) of the fit, **(h)** the Q/Q_{exp} for each point in time, and **(i)** the Q/Q_{exp} values for each ion.

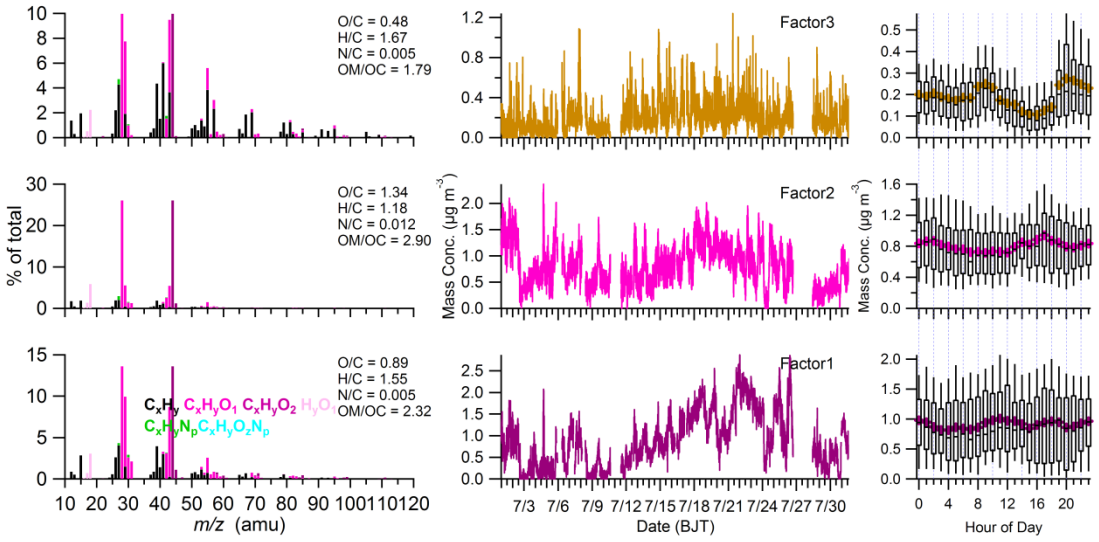

Figure ~~S2~~S4. The 3-factor solution PMF results: **(left)** high-resolution mass spectrum of three OA factors colored by six ion categories at m/z < 120, **(middle)** time series of the three OA factors, and **(right)** diurnal variations of mass concentrations of the three OA factors (the whiskers above and below the boxes indicate the 90th and 10th percentiles, the upper and lower boundaries respectively indicate the 75th and 25th percentiles, the lines in the boxes indicate the median values, and the cross symbols indicate the mean values).

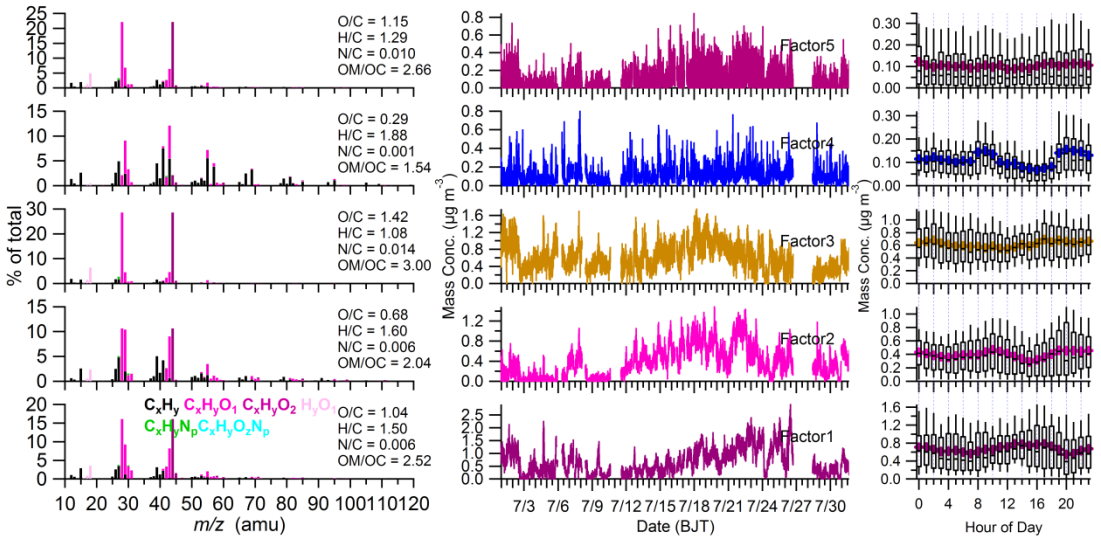

20 **Figure ~~S3~~S5.** The 5-factor solution PMF results: **(left)** high-resolution mass spectrum of five OA factors colored by six ion categories at m/z < 120, **(middle)** time series of the five OA factors, and **(right)** diurnal variations of mass concentrations of the five OA factors (the whiskers above and below the boxes indicate the 90th and 10th percentiles, the upper and lower boundaries respectively indicate the 75th and 25th percentiles, the lines in the boxes indicate the median values, and the cross symbols indicate the mean values).

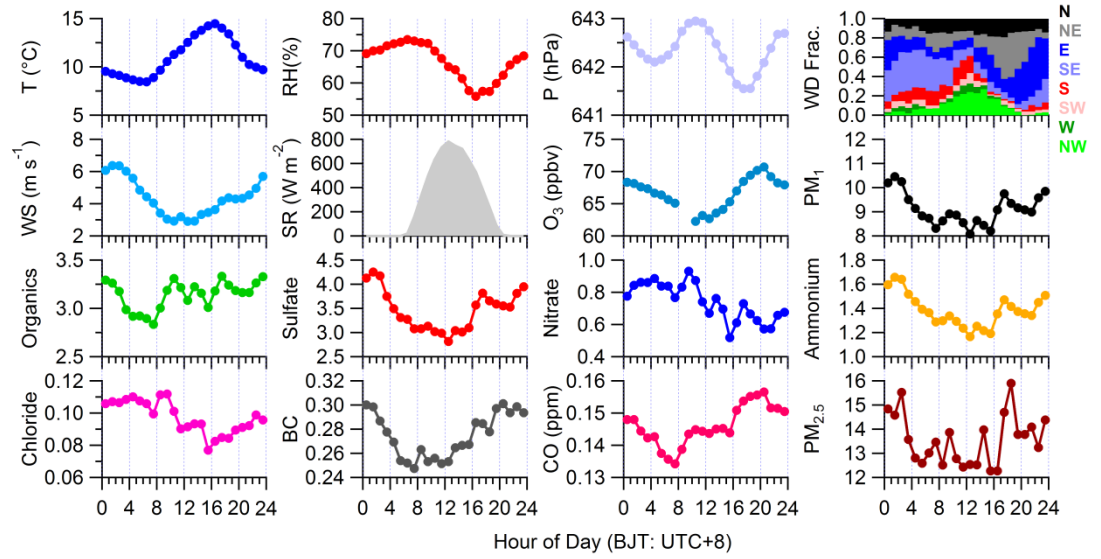

25 **Figure ~~S4~~S6.** Diurnal variations of meteorological conditions, PM_1 chemical species and other relevant gaseous and particulate parameters.

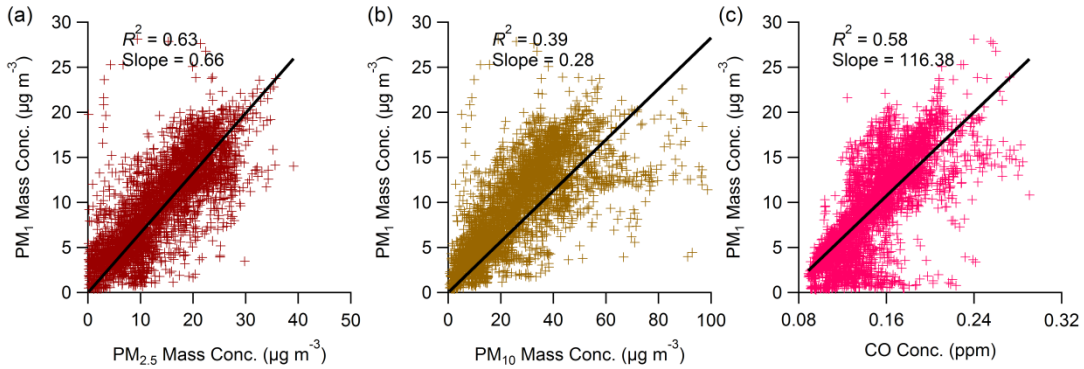

Figure ~~S5~~S7. Scatterplots of mass concentrations of **(a)** PM_1 vs. $PM_{2.5}$, **(b)** PM_1 vs. PM_{10}, and **(c)** PM_1 vs. CO in this study.

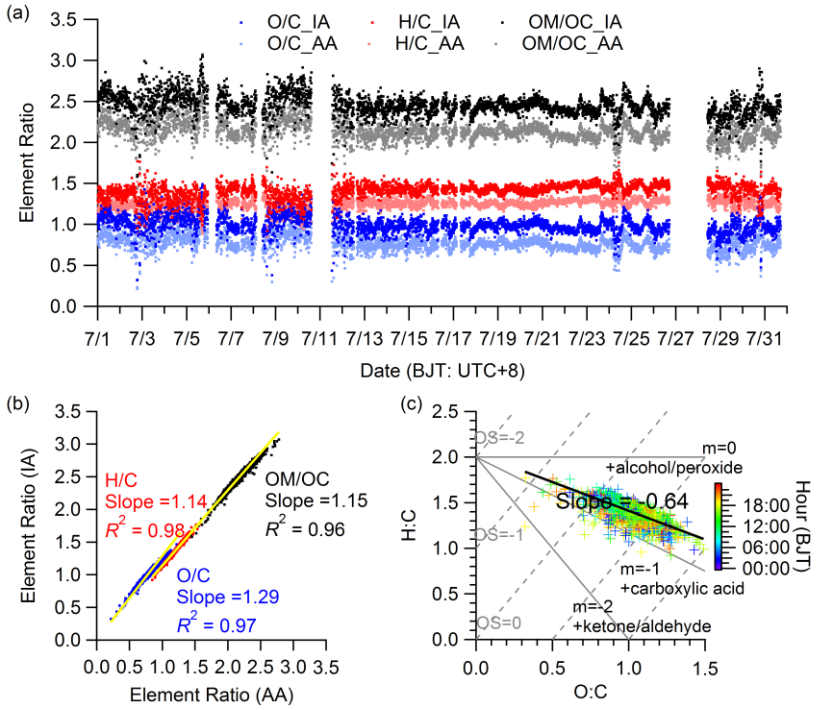

Figure ~~S6~~S8. (a) Comparison of the temporal variations of O/C, H/C, and OM/OC ratios using "Improved-ambient" method versus "Aiken ambient" method for the whole study period, **(b)** scatterplot of elemental ratios with "Improved-ambient" method versus that with "Aiken ambient" method and **(c)** Van Krevelen diagram of H/C versus O/C for OA in this study.

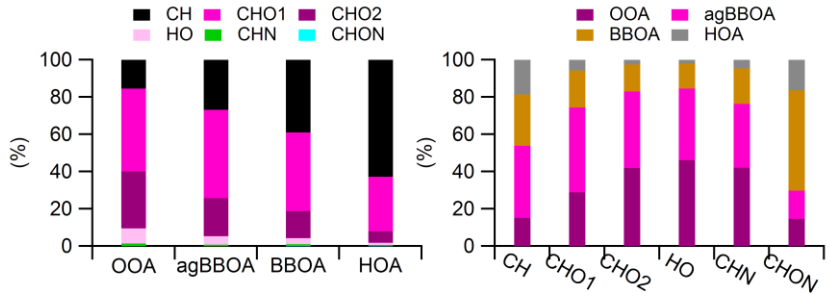

Figure ~~S7~~S9. The contributions of **(left)** six ionic categories to PMF factors and **(right)** PMF factors to six ionic categories.

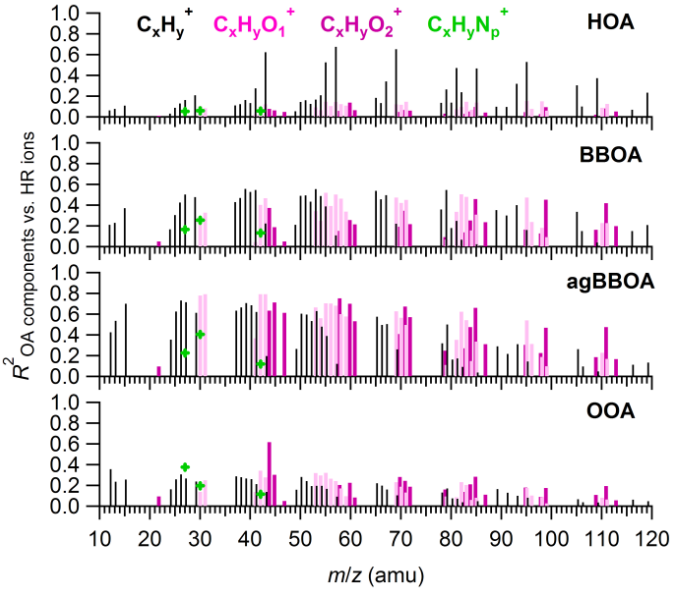

Figure ~~S8~~S10. Correlations between each organic component and HRMS ions colored by four ion categories ($C_xH_y^+$, $C_xH_yO^+$, $C_xH_yO_2^+$, $C_xH_yN_p^+$).

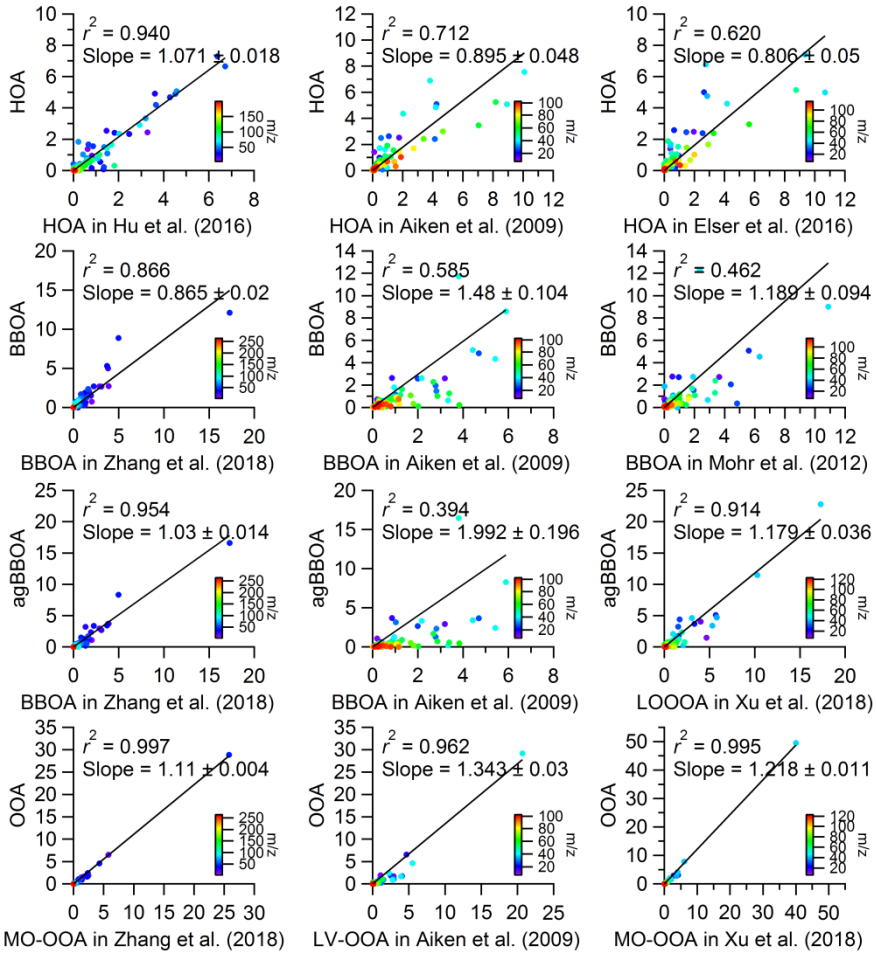

40 **Figure ~~S9~~S11.** Scatter plots of the comparisons between the four high-resolution mass ~~spectrums~~ spectra identified in this study and those high-resolution mass ~~spectrums~~ spectra determined from other studies.

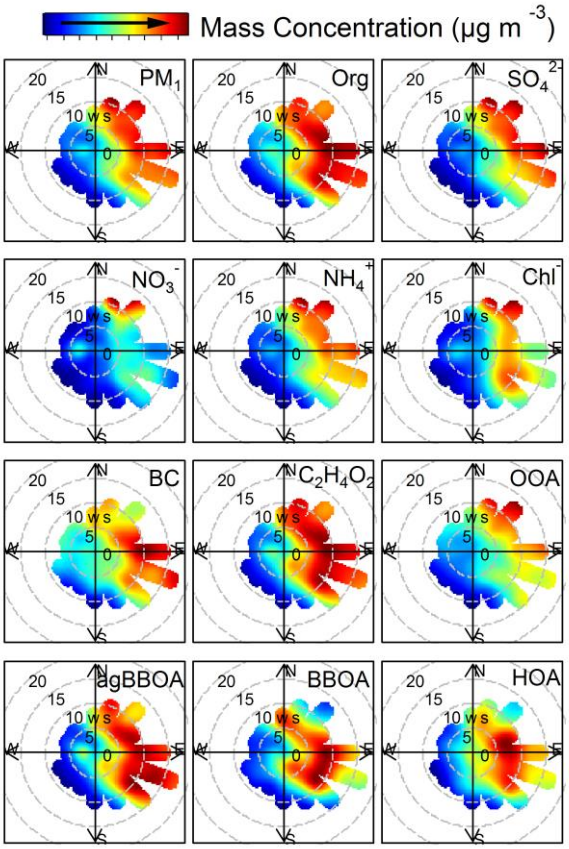

Figure ~~S10~~S12. Bivariate polar plots that illustrate the variations of mass concentrations (colored) of each PM_1 species and organic components as a function of wind speed (m s^{-1}) and wind direction in this study.

References

Aiken, A. C., Salcedo, D., Cubison, M. J., Huffman, J. A., DeCarlo, P. F., Ulbrich, I. M., Docherty, K. S., Sueper, D., Kimmel, J. R., Worsnop, D. R., Trimborn, A., Northway, M., Stone, E. A., Schauer, J. J., Volkamer, R. M., Fortner, E., de Foy, B., Wang, J., Laskin, A., Shutthanandan, V., Zheng, J., Zhang, R., Gaffney, J., Marley, N. A., Paredes-Miranda, G., Arnott, W. P., Molina, L. T., Sosa, G., and Jimenez, J. L.: Mexico City aerosol analysis during MILAGRO using high resolution aerosol mass spectrometry at the urban supersite (T0)–Part 1: Fine particle composition and organic source apportionment, Atmos. Chem. Phys., 9, 6633-6653, doi:10.5194/acp-9-6633-2009, 2009.

Du, W., Sun, Y. L., Xu, Y. S., Jiang, Q., Wang, Q. Q., Yang, W., Wang, F., Bai, Z. P., Zhao, X. D., and Yang, Y. C.: Chemical characterization of submicron aerosol and particle growth events at a national background site (3295 m a.s.l.) on the Tibetan Plateau, Atmos. Chem. Phys., 15, 10811-10824, doi:10.5194/acp-15-10811-2015, 2015.

Elser, M., Huang, R.-J., Wolf, R., Slowik, J. G., Wang, Q., Canonaco, F., Li, G., Bozzetti, C., Daellenbach, K. R., Huang, Y., Zhang, R., Li, Z., Cao, J., Baltensperger, U., El-Haddad, I., and Prévôt, A. S. H.: New insights into PM_{2.5} chemical composition and sources in two major cities in China during extreme haze events using aerosol mass spectrometry, Atmos. Chem. Phys., 16, 3207-3225, doi:10.5194/acp-16-3207-2016, 2016.

Hu, W. W., Hu, M., Hu, W., Jimenez, J. L., Yuan, B., Chen, W., Wang, M., Wu, Y., Chen, C., Wang, Z., Peng, J., Zeng, L., and Shao, M.: Chemical composition, sources, and aging process of submicron aerosols in Beijing: Contrast between summer and winter, J. Geophys. Res. Atmos., 121, 1955-1977, doi:10.1002/2015jd024020, 2016.

Mohr, C., DeCarlo, P. F., Heringa, M. F., Chirico, R., Slowik, J. G., Richter, R., Reche, C., Alastuey, A., Querol, X., Seco, R., Peñuelas, J., Jiménez, J. L., Crippa, M., Zimmermann, R., Baltensperger, U., and Prévôt, A. S. H.: Identification and quantification of organic aerosol from cooking and other sources in Barcelona using aerosol mass spectrometer data, Atmos. Chem. Phys., 12, 1649-1665, doi:10.5194/acp-12-1649-2012, 2012.

Wang, J., Zhang, Q., Chen, M., Collier, S., Zhou, S., Ge, X., Xu, J., Shi, J., Xie, C., Hu, J., Ge, S., Sun, Y., and Coe, H.: First Chemical Characterization of Refractory Black Carbon Aerosols and Associated Coatings over the Tibetan Plateau (4730 m a.s.l), Environ. Sci. Technol., 51, 14072-14082, doi:10.1021/acs.est.7b03973, 2017.

Xu, J., Zhang, Q., Shi, J., Ge, X., Xie, C., Wang, J., Kang, S., Zhang, R., and Wang, Y.: Chemical characteristics of submicron particles at the central Tibetan Plateau: insights from aerosol mass spectrometry, Atmos. Chem. Phys., 18, 427-443, doi:10.5194/acp-18-427-2018, 2018.

Zhang, X., Xu, J., Kang, S., Liu, Y., and Zhang, Q.: Chemical characterization of long-range transport biomass burning emissions to the Himalayas: insights from high-resolution aerosol mass spectrometry, Atmos. Chem. Phys., 18, 4617-4638, doi:10.5194/acp-18-4617-2018, 2018.

Zheng, J., Hu, M., Du, Z., Shang, D., Gong, Z., Qin, Y., Fang, J., Gu, F., Li, M., Peng, J., Li, J., Zhang, Y., Huang, X., He, L., Wu, Y., and Guo, S.: Influence of biomass burning from South Asia at a high-altitude mountain receptor site in China, Atmos. Chem. Phys., 17, 6853-6864, doi:10.5194/acp-17-6853-2017, 2017.